INSTITUTO POLITÉCNICO DE LISBOA

ESCOLA SUPERIOR DE TECNOLOGIA DA SAÚDE DE LISBOA

SYNTHESIS OPTIMIZATION OF [^{11}C]PITTSBURGH COMPOUND B BY THE CAPTIVE SOLVENT METHOD

GONÇALO DOS SANTOS CLEMENTE

ANTERO DE ABRUNHOSA, PhD (ICNAS/IBILI)

Mestrado em Medicina Nuclear

Lisboa, 2013

INSTITUTO POLITÉCNICO DE LISBOA

ESCOLA SUPERIOR DE TECNOLOGIA DA SAÚDE DE LISBOA

SYNTHESIS OPTIMIZATION OF [^{11}C]PITTSBURGH COMPOUND B BY THE CAPTIVE SOLVENT METHOD

GONÇALO DOS SANTOS CLEMENTE

ANTERO DE ABRUNHOSA, PhD (ICNAS/IBILI)

Mestrado em Medicina Nuclear

(esta versão incluiu as críticas e sugestões feitas pelo júri)

Lisboa, 2013

Acknowledgements

During the time I took to complete this work I was fortunate enough to count on the support of many people who readily agreed to cooperate.

I would like to start by thanking the Institute for Nuclear Sciences Applied to Health, in the name of its director Miguel Castelo-Branco MD/PhD, for providing me with access to facilities, equipment and optimal conditions for the development of this work.

I thank Antero Abrunhosa PhD, for agreeing to supervise this project, giving me complete freedom of action and autonomy, and whose support was crucial in all phases of the developed work.

To Vítor Alves for his tremendous fellowship, dedication, hard work and electrotechnical support without which everything would have been much more difficult. He was an indispensable part in the development of this project.

I thank Francisco Alves PhD, and Sérgio do Carmo PhD, that always with their characteristic good humour were essential in the cyclotron operating procedures.

And finally, I could not forget to thank my colleagues João Oterelo, Ricardo Faustino and Pedro Lopes for their friendship and tireless encouragement.

A thank to all those who, in one way or another, directly or indirectly, helped me get through every challenge.

Abstract

Alzheimer's disease (AD), the most prevalent type of dementia, is a condition that leads to a progressive and irreversible deterioration of predominantly cortical functions. AD is characterized by loss of mental faculties, memory impairment, spatial and temporal disorientation, confusion and reasoning difficulties. The clinical signs of AD occur in parallel or are even preceded by intra or extracellular abnormal accumulation of amyloid beta (Aβ) deposits, Aβ toxic oligomers and τ protein neurofibrillary tangles in brain tissue. For this reason, molecular imaging studies with radiotracers that target Aβ can provide an important tool not only to detect the onset of the disease but also to assess the potential of new therapeutic approaches. Carbon-11 labelled Pittsburgh Compound B ([^{11}C]PiB) binds *in vivo* to Aβ and is nowadays established in literature as the reference radiotracer for AD due to its higher sensitivity and good specificity for earlier detection of the disease.

The aim of this work was to optimize a simple, rapid and fully automated preparation of [^{11}C]PiB based on the captive solvent method. Starting from [^{11}C]CO_2 produced in a cyclotron through the ^{14}N(p,α)^{11}C nuclear reaction, a final sterile, non-pyrogenic saline solution of [^{11}C]PiB was produced with high quality and reproducibility using a series of automated modules.

The specific activity of the [^{11}C]PiB produced was 27.6±4.1 GBq/μmol and radiochemical purity was always above 98%. Residual ethanol and acetonitrile in the solution were controlled using gas chromatography. pH, radionuclidic purity and half-life were all within their pharmacopoeia values.

Keywords: [^{11}C]Pittsburgh Compound B; [^{11}C]methyl triflate; captive solvent method; Alzheimer's disease.

Resumo

A doença de Alzheimer (AD), o tipo mais prevalente de demência, conduz a uma deterioração progressiva e irreversível de funções predominantemente corticais. A AD caracteriza–se por perda das faculdades mentais, perturbações da memória, desorientação espacial e temporal, confusão e problemas de raciocínio. Os sinais clínicos de AD ocorrem em paralelo, ou são mesmo precedidos, de depósitos anómalos, intra ou extracelulares, de placas β-amilóides (Aβ) e emaranhados neurofibrilares de proteína τ no tecido cerebral. Por este motivo, os estudos de imagiologia molecular utilizando radiotraçadores com afinidade para os depósitos de Aβ são uma ferramenta indispensável no diagnóstico precoce das demências, na avaliação da resposta a novas terapêuticas e no auxílio ao desenvolvimento de terapias de última geração. O Composto B de Pittsburgh marcado com carbono-11 ([^{11}C]PiB) liga-se *in vivo* aos depósitos de Aβ e está actualmente bem estabelecido na literatura como o radiotraçador de referência para AD devido à sua elevada sensibilidade e boa especificidade na detecção precoce desta demência.

O objectivo deste trabalho foi de, partindo do [^{11}C]CO_2 produzido em ciclotrão através da reacção nuclear ^{14}N(p,α)^{11}C, optimizar um método automático, rápido e simplificado de preparação de uma solução estéril e apirogénica de [^{11}C]PiB baseado no método de captura de solvente.

A actividade específica obtida foi de cerca de 27.6±4.1 GBq/μmol e a pureza radioquímica esteve sempre acima dos 98%. Os níveis residuais de etanol e acetonitrilo foram controlados por cromatografia gasosa. O pH, a pureza radionuclídica e o período de semi-desintegração estavam todos dentro dos respectivos valores de referência.

Palavras-chave: Composto B de Pittsburgh; triflato de [^{11}C]metilo; metilação em *loop*; Doença de Alzheimer.

List of abreviations

AD – Alzheimer's disease

Ah – Ampere

APP – Amyloid precursor protein

Aβ – Amyloid beta

BBB – Blood-brain barrier

BPT – Bubble point test

Bq – Becquerel

BTA – Benzothiazole

cGRPP – Current Good Radiopharmacy Practices

Ci – Curie

CT – Computed Tomography

DC – Decay corrected

DMF – Dimethylformamide

DMSO – Dimethyl sulfoxide

ESTeSL – Escola Superior de Tecnologia da Saúde (Lisbon Higher Scool of Health Technology)

EU – Endotoxyns units

FDG – Fluorodeoxyglucose

FID – Flame ionization detector

g – Gram

GC – Gas chromatography

GLP – Good Laboratory Practices

GMP – Good Manufacturing Practices

HPLC – High Pressure Liquid Chromatography

i.v. – Intravenous

ICNAS – Instituto de Ciências Nucleares Aplicada à Saúde (Institute for Nuclear Sciences Applied to Health)

l – Liter

LAL – *Limulus* amebocyte lysate

LD – Lethal dosis

m – Meter

M – Molar

MCI – Mild cognitive impairment

Me – Methyl

MEK – Methyl ethyl ketone

MeV – Mega electron-volt

min – Minute

MM – Molecular mass

MOMO – Methoxymethyl

MRI – Magnetic Resonance Imaging

N – Normal

OECD – Organization for Economic Cooperation and Development

PET – Positron Emission Tomography

Ph. Eur. – European Pharmacopoeia

PiB – Pittsburgh Compound B

ppm – Particles per million

R_t – Retention time

SA – Specific activity

SN – Nucleophilic substitution

SPE – Solid Phase Extraction

SPECT – Single Photon Emission Computed Tomography

Tf - Triflate

THF – Tetrahydrofuran

UV – Ultraviolet

WFI – Water for injections

Table of contents

Acknowledgements ..... *iii*
Abstract ..... *v*
Resumo ..... *vii*
List of abreviations ..... *ix*
Table of contents ..... *xi*
List of tables ..... *xiii*
List of figures ..... *xv*

1. Introduction **1**
2. Literature review **3**
2.1 Molecular mechanisms of Alzheimer's disease 4
2.2 Molecular Imaging in Alzheimer's disease 7
2.2.1 [^{11}C]PiB in the differentiation of Alzheimer's disease 11
2.3 Synthesis of short lived PET radiotracers 13
2.3.1. Carbon-11 radiochemistry 16
2.3.2 Pittsburgh Compound B radiosynthesis 20
3. Justification of the project **23**
4. Methodology **25**
4.1 Instruments and materials 26
4.2 Experimental procedures 27
4.2.1 Optimization of the chromatographic conditions 28
4.2.2 Production of [^{11}C]CH_3I and [^{11}C]CH_3OTf 28
4.2.3 Production of [^{11}C]PiB in a captive solvent loop 31
4.2.4 Purification and reformulation of the final product 32
4.2.5 Quality control 33
5. Results and discussion **35**
5.1 Chromatographic system 35
5.2 Synthesis of [^{11}C]CH_3I and conversion into [^{11}C]CH_3OTf 38
5.3 The reaction by the captive solvent method 43
5.4 Final purified saline solution of [^{11}C]PiB 48
5.5 Assurance of the final product quality 51
6. Final considerations **57**
7. References **61**

List of tables

Table 2.1. Main radiotracers for neuroimaging with PET and SPECT. 8
Table 2.2. Features of most commonly used PET radionuclides. 13
Table 5.1. $LiAlH_4$ volume influence in [^{11}C]CO_2 trap and [^{11}C]CH_3I production. 40
Table 5.2. Precursor dilution influence in [^{11}C]PiB reaction yield and specific activity.. 46
Table 5.3. Reaction time influence in [^{11}C]PiB production yield and specific activity. .. 47
Table 5.4. Optimal [^{11}C]PiB reaction conditions and comparison with several authors. 47
Table 5.5. Results obtained with [^{11}C]PiB radiolabellings. 52

List of figures

Figure 2.1. The amyloid cascade hypothesis. 5
Figure 2.2. Flow chart for evaluation of PET brain studies..... 10
Figure 2.3. Progression of Aβ deposits in AD. 12
Figure 2.4. Pathway from cyclotron production to final use of a PET tracer. 14
Figure 2.5. Radioactive precursors for ^{11}C synthesis. 17
Figure 2.6. Scheme of loop injector as a solid phase reaction system. 19
Figure 2.7. Structure of thioflavin T analogues and radiolabelling reactions. 21
Figure 4.1. Scheme of the adopted [^{11}C]PiB synthesis process. 25
Figure 4.2. Diagram of the interactions between the devices involved. 26
Figure 4.3. Schematic diagram of the automated ^{11}C radiolabelling system used. 28
Figure 4.4. Columns used on the synthesis of [^{11}C]CH_3OTf..... 31
Figure 5.1. Analytical HPLC of cold standards mixture. 37
Figure 5.2. Semi-preparative HPLC of cold standards mixture. 37
Figure 5.3. Reference curve for the calculation of PiB concentration. 38
Figure 5.4. Synthesis of [^{11}C]CH_3I by the “wet method”. 39
Figure 5.5. [^{11}C]CH_3I production profile. 41
Figure 5.6. Semi-preparative HPLC of [^{11}C]PiB and main radiochemical impurities. 42
Figure 5.7. Optimum profile for [^{11}C]CH_3OTf trapping in the loop..... 44
Figure 5.8. Semi-preparative HPLC of [^{11}C]PiB methylation using DMSO. 45
Figure 5.9. Semi-preparative HPLC for purification of [^{11}C]PiB. 48
Figure 5.10. SPE C18 cartridge profile during [^{11}C]PiB purification. 49
Figure 5.11. Gas chromatography of the final [^{11}C]PiB i.v. solution. 53
Figure 5.12. Analytical HPLC of [^{11}C]PiB solution before purification. 54
Figure 5.13. Analytical HPLC of the final [^{11}C]PiB i.v. solution. 54
Figure 5.14. [^{11}C]PiB final solution stability over time. 55
Figure 6.1. [^{11}C]PiB amyloid binding to the brain of an AD and healthy cases. 59

1. Introduction

This dissertation is submitted for the fulfilment of the requirements for the Master's degree in Nuclear Medicine, specialization in Radiopharmacy, by the Lisbon Higher School of Health Technology (ESTeSL). The work was conducted at the Institute for Nuclear Sciences Applied to Health (ICNAS), University of Coimbra, with the overall aim of establishing an automated and reproducible method for radiolabelling - by the captive solvent method -, purification and reformulation of [^{11}C]Pittsburgh Compound B ([^{11}C]PiB) using a system composed by commercial synthesis modules (Bioscan Inc. Washington DC, USA) in order to obtain a sterile and pyrogen-free injectable solution.

Originally developed in 2000 at the University of Pittsburgh, [^{11}C]PiB is a benzothiazole compound, analogue of thioflavin T, with known affinity for amyloid beta (Aβ) deposits. The compound is labelled with the positron emitter carbon-11 ([^{11}C]) for the early diagnosis of Alzheimer's disease (AD) with Positron Emission Tomography (PET). PET is a non-invasive Nuclear Medicine diagnostic technique which can reconstruct functional images through information generated from the two anti-parallel 511 keV γ photons emitted by annihilation of an emitted positron with an electron of the surrounding material.

AD is manifested by a progressive deterioration of mental and intellectual faculties that interfere with the ability to function normally in society. It is also characterized by a deterioration of both long and short term memories and a disintegration of the personality due to changes in the discernment and judgment. Being associated with advancing age and considering the world demographic development for the coming decades, that predicts a dramatic increase in the population aged over 65 years, it is expected that AD will become a major health concern in the coming years. It is, therefore, of great importance the development of diagnostic techniques that target the Aβ plaques, the hallmark of this dementia. Currently there is no clinical or laboratory exam that can, by itself, definitively diagnose AD in life. The only way to do this is through direct observation of the presence of amyloid plaques in cerebral homogenates after autopsy. Nevertheless, several studies published in the literature demonstrate a strong quantitative correlation between the presence of these deposits and *in vivo* uptake of [^{11}C]PiB. This has consolidated this radiotracer as a powerful tool with high sensitivity and specificity for validating treatments for neurodegenerative diseases and opens a window to a new era of preventive medicine in dementia. Using this tracer it

will be possible to test new drugs at an early stage of the disease, even before the symptoms begin to manifest.

Owing to its physicochemical characteristics, the use of radiotracers labelled with ^{11}C in routine PET scans requires the presence *in loco* of a suitable production facility. The only centre in Portugal that hosts a biomedical cyclotron, a radiochemistry laboratory and a PET diagnostic unit is ICNAS. Considering that pre-validated kits for routine production of [^{11}C]PiB are not available, each production facility has to develop an automated synthesis, purification and dispensing process based on multi-purpose hardware available. The development of such process is the subject of this work and the [^{11}C]PiB produced is expected to make a strong impact on the diagnosis and clinical management of AD in Portugal and provide an important tool for basic and clinical for R&D in this area.

The work plan included a revision of the state-of-the-art in the field including molecular basis of AD and its diagnosis as well as major challenges faced by the radiolabelling of products with ^{11}C and its automation. Technical challenges to overcome included the used of automated modules and the understanding of electromechanical processes necessary for its operation and correct maintenance. The main experimental work was then the implementation and optimization of the [^{11}C]PiB synthesis, purification and reformulation specially in regards to the main parameters of purity (chemical and radiochemical), yield and specific activity (SA) of the final product.

Following the so called “wet method” the process starts from cyclotron produced carbon dioxide ([^{11}C]CO_2), obtained by a $^{14}N(p,\alpha)^{11}C$ nuclear reaction through the irradiation of a gaseous nitrogen target with 0.5% of O_2. Subsequently, [^{11}C]CO_2 produced will be converted on an automated system (MeI-Plus™, Bioscan Inc.) to [^{11}C]methyl iodide ([^{11}C]CH_3I) and [^{11}C]methyl triflate ([^{11}C]CH_3OTf). The reaction then takes place by the “captive solvent” methylation loop technique (AutoLoop™, Bioscan Inc.) and, after semi-preparative High Pressure Liquid Chromatography (HPLC) purification, final reformulation is done (ReFORM-Plus™, Bioscan Inc.) to produce [^{11}C]PiB in a suitable solution for *in vivo* human studies.

Due to short half-life of ^{11}C (20.4 minutes) the greatest challenge is the promptitude by which the radiotracer must be synthesized, purified and quality controlled before administration is carry out. It is, therefore, very important that the entire process of synthesis and evaluation of the radiopharmaceutical is as fast as possible. This is a critical factor that has to be taken into account in all steps of the optimization process.

2. Literature review

It was in the 1960s that various socio-economic studies began to draw attention to the demographic phenomenon of aging. Studies of the Organization for Economic Cooperation and Development (OECD) estimate that in 2050 one fifth of the world population will have more than 65 years[1]. As a first approach to this problem we can expect that this aging will be based on an increase of average life expectancy which announces a better improvement of medical techniques and an enlargement to the access to specialized platforms that ensures a continuum health care to the population, but on the other hand this factor will increase the risk for developing chronic and degenerative complications, of which one of the most important group are neurodegenerative diseases or dementias.

In 2011 the Alzheimer's disease International estimated a total of 36 million people suffering from dementia worldwide, representing an economic cost exceeding 1% of the world total Gross Domestic Product. This number is expected to rise to 66 million by 2030 and 115 million by 2050[2]. A project from European Collaboration on Dementia group estimated about 153.000 persons suffering from dementia in Portugal, of which 90.000 have AD. This numbers are also expected to double in the next 20 years.

AD is the most prevalent type of dementia, i.e., a disease that leads to progressive and irreversible deterioration of predominantly cortical functions, and is characterized by loss of mental faculties, memory impairment, spatial and temporal disorientation, confusion and reasoning problems[3]. These symptoms worsen as the neurodegenerative process is intensified and the communication between neurons becomes deficient which culminates in behaviour and personality changes and inability to complete routine activities. The visible signs of AD occur in parallel or are even preceded by intra or extracellular abnormal accumulation of Aβ deposits, Aβ toxic oligomers and τ proteins neurofibrillary tangles in nerve cells[4]. The study of these changes at a molecular level became a strong line of scientific research in order to lead to a better understanding of the underlying mechanisms of this dementia, to identify new biomarkers and to develop resources to support their diagnosis at an earlier time, a strategy that has the potential to increase the efficiency of the therapeutics.

For this reason, molecular imaging studies with radiotracers that target Aβ can provide an important tool not only to detect the onset of the disease but also to assess the potential of new therapeutic approaches.

2.1 Molecular mechanisms of Alzheimer's disease

Cerebral regions involved in learning, attention and memory processes, including frontal and temporal lobes, are anatomically diminished in AD patients due to neuronal death and synaptic degeneration[4]. Other modifications, such as a decrease in astrocytes, proliferation of abnormal clusters of microglial cells (that produce a number of various neurotoxic substances) and a reduction in acetylcholinesterase levels and cholinergic neuroreceptors, associated with brain regions involved in processes related with learning and memory, were also associated to this dementia[5-7]. However, since other dementias share many of the symptoms and neurological alterations of AD, such as frontotemporal, Lewy body or multi-infarct, its diagnosis was only definitely closed when Aβ plaques and neurofibrillary tangles were identified in post-mortem brain tissue[8]. These two histopathological hallmarks of AD are directly related to the progressive loss of inter-neuronal communications as firstly described in early XX century by German neurologist Alois Alzheimer after an anatomopathological examination of the brain of a patient who presented abnormal behaviour[9].

Nowadays it is known that Aβ peptides derive from the amyloid precursor protein (APP) that plays an important role on neuronal development and in the adherence of neurons to the cellular matrix. APP is transported through the axons to the synaptic terminals where is accumulated at high concentrations. Throughout this transport it suffers several proteolytic cleavages originating Aβ peptides. Normally these Aβ peptides are physiologically removed from brain parenchyma but, in AD, several mutations or failures in the clearance mechanisms are thought to exist (e.g., non activated microglia) that result in an abnormal progressive accumulation of Aβ oligomers[7, 10]. The neurotoxicity of these protein deposits with β-sheet structure were already verified by *in vitro* studies and probably are the primarily cause that leads to the formation of amyloid plaques which originate modifications in synaptic plasticity and neuronal integrity[11-13]. This cascade culminates in neurodegeneration through processes such as oxidative stress, disturbances in energetic metabolism due to deterioration of glucose transport mechanisms, modifications in cellular calcium homeostasis or adulteration of synaptic proteins such as τ protein[14].

As a result of the changes produced during the amyloid cascade, and in addition to the Aβ plaques, neurofibrillary tangles of accumulated τ proteins are also formed (see Figure 2.1). These soluble proteins are usually responsible for tubulin polymerization and the aggregation of microtubules, an essential process in the

formation of the cytoskeleton[15-17]. Nevertheless, when in the form of neurofibrillary tangles, τ proteins become insoluble, phosphorylated and unstable decreasing their affinity to microtubules. This originates cytoskeleton rupture and, consequently, neuronal destruction[18, 19]. The mechanism that triggers these reactions it is not yet totally known but there are evidences who suggests that the deposition of Aβ oligomers adulterates the activity of some kinases (FAK1, PTK2, CDK5, GSK3α) that will promote the abnormal phosphorylation of τ protein[10].

About 70% of suspected AD cases are attributed to genetic causes. Dominant mutations in genes that encode APP, presenilin or apolipoprotein E are among the most frequently found risk factors[20]. Other genes presenting a risk for AD still remain the subject of numerous studies[21]. Mutations in τ proteins are mainly responsible for frontotemporal dementia and corticobasal degenerations and are not an AD risk factor[22]. Nevertheless, their study remains important because, although the presence of Aβ plaques is the hallmark of AD, the severity of the disease is more closely related with the presence of the neurofibrillary tangles of τ proteins[23].

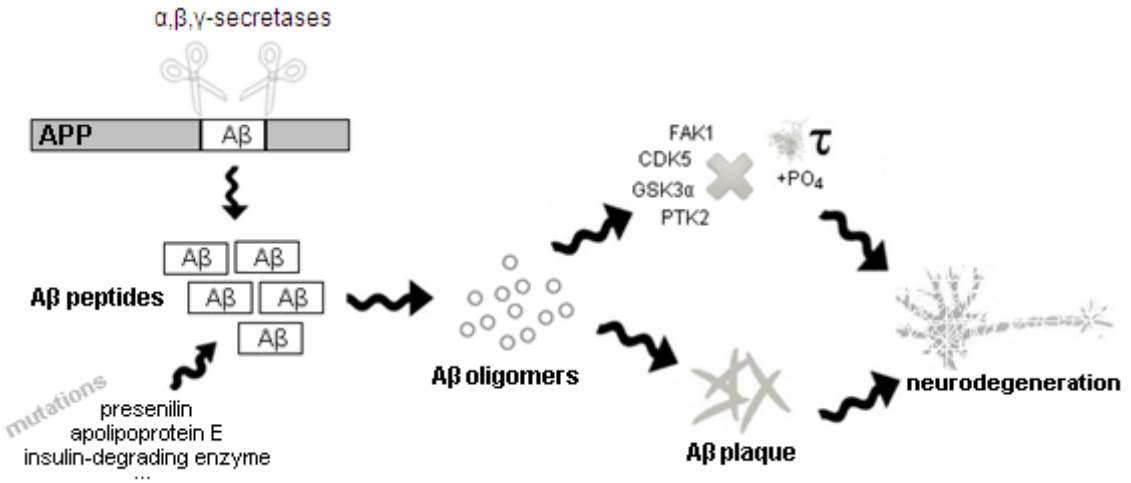

Figure 2.1. The amyloid cascade hypothesis.

There is no single medical test that can unequivocally diagnose AD in life. Therefore, the diagnosis is performed by a multidisciplinary approach using neuropsychological tests, blood and cerebrospinal fluid analysis, electroencephalograms and structural neuroimaging techniques through a process of exclusion of other pathologies that could

have similar signs and symptoms[24]. Within the neuroimaging techniques, Computed Tomography (CT) and Magnetic Resonance Imaging (MRI) are, in general, routinely used in the study of patients with suspected dementia to exclude other clinical causes such as tumours, cerebral haematomas, hydrocephaly or cerebrovascular diseases[25].

The advantage of CT scanning is debatable since its efficiency to reveal abnormalities that were not described in previous clinical examinations is only between 1% and 10%[26, 27]. Due to its increased specificity, MRI became the reference imaging technique to reveal atrophies in hippocampus, posterior cerebral cortex and in the intermediate region between temporal and parietal lobes in patients with suspected AD[28]. In the absence of a curative or preventive treatment for AD, an early diagnosis allows a non-pharmacological and pharmacological intervention more effective in relieving symptoms and preserving physical skills, with real gains in quality of life. For this reason it is important to diagnose AD at an early stage when no anatomic effects are present yet. So, an imaging technique with focus on the very first molecular changes will be capable to improve prophylaxis and be a valuable resource on the search for new drugs capable to stop or slow down these processes.

The diagnostic procedures in Nuclear Medicine by Single Photon Emission Computed Tomography (SPECT) and especially PET, which in the last decade has been focus of major interest and scientific development associated with the increase of available radiotracers, allow *in vivo* imaging of brain activity by mapping blood flow or glucose metabolism, enable the study of cerebral biochemistry and neurotransmitters and provide differential diagnosis for some dementias[29, 30].

Molecular imaging with PET associated with suitable radiotracers provides valuable information about many aspects of the neurobiology of AD and has potential application in early diagnosis and to monitor therapeutic efficiency. Until recently, the most used diagnostic criteria for AD using functional imaging has been the identification of spots with reduced glucose metabolism in parieto-temporal cerebral areas. This studies use [^{18}F]fluorodeoxyglucose ([^{18}F]FDG) and have a sensibility and specificity of 86%[31]. However the development of new specific radiotracers for Aβ deposits, simultaneously with results that showed a strong quantitative correlation between *in vivo* uptake and the presence of these Aβ plaques detected post-mortem in brain tissue, has increased the interest in their clinical use for a faster and more accurate diagnosis and differentiation of dementias.

2.2 Molecular Imaging in Alzheimer's disease

Nuclear Medicine can be defined as the use of radioisotopes for the diagnosis, treatment and study of diseases, being one of the most relevant techniques in the emerging field of Molecular Imaging which allows the visualization, characterization and quantification of the molecular scale cellular and biochemical processes in living systems[32, 33]. The major challenge of brain molecular imaging is to develop radiotracers that penetrate in the highly selective blood-brain barrier (BBB). For this, they should not have very high molecular weight (less than 600 Dalton), be neutral or have a weak ionization at physiological pH and present low percentage of plasma protein binding. It is also important that they have a high SA and are not metabolized, during the time of the imaging acquisition, to active compounds that could mask the specific signal of the parent compound[34-36]. To have a radiotracer that effectively cross the BBB it is necessary to reach a compromise between lipophilicity and hydrophilicity since if it is too lipophilic will tend to be trapped in the adipose tissues, to bind more tightly to plasma proteins, which will decrease the interaction with receptors, and to be slightly soluble in aqueous phases, which alters the desired biodistribution. By the other way, if the radiotracer is very hydrophilic it may not be able to pass through membranes, including BBB, increasing the susceptibility of being rapidly excreted before reaching the desired target[37].

In general we can consider, in the clinical setting, four classes of radiotracers for functional brain imaging. Those include the study of blood flow, glucose metabolism, receptor mapping and the characteristic biomarkers of a particular dementia[33]. Currently there is a growing availability of radiolabelled molecules with specificity to picomolar scale neuronal mechanisms. These are used in pre-clinical studies and in research with the aim of reaching an increasingly early diagnosis of dementias, to evaluate the response to new therapies and to help in the development of last generation psychoactive drugs. Table 2.1 lists some of the most used SPECT and PET radiotracers for neurologic and psychiatric nuclear imaging studies[29, 30, 33, 38].

Cerebral blood flow is directly related to the supply of metabolic nutrients to neurons. For this reason, it is important to study this factor to map which brain regions show a deficit of perfusion and correlate them with the symptoms presented by patients with dementia. ^{99m}Tc-ECD and ^{99m}TC-HMPAO are two agents that diffuse to cerebral tissue and suffer an intracellular retention proportional to blood flow. This phenomenon can be correlated with AD since cerebral perfusion has different patterns depending on the

type of dementia[29, 39]. By studying its uptake in the occipital and parietal cortices, [^{123}I]iodoamphetamine has also been used for the differential diagnosis between AD and multi-infarct dementia[40]. The use of SPECT radiotracers which allow the study of the BBB integrity, such as [^{67}Ga] gallium citrate, has also proved to be important in the understanding of AD since there is some evidence that relate the destruction of BBB with an increased cerebral deposition of Aβ oligomers[41].

Table 2.1. Main radiotracers for neuroimaging with PET and SPECT

Biological Process	Target	Radiotracers	
		SPECT	**PET**
Cerebral blood flow		^{99m}Tc-HMPAO; ^{99m}TC-ECD; [^{123}I]iodoamphetamine	[^{15}O]H_2O
BBB integrity		^{99m}Tc-glucoheptonate; [^{67}Ga]gallium citrate; $^{99m}TcO_4^-$;	
Glucose metabolism	Hexokinase and glucose transporters		[^{18}F]FDG
Neurotransmitters	Dopaminergic system	[^{123}I] β-CIT; ^{99m}Tc-TRODAT; [^{123}I]IBZM; [^{123}I]altropane	[^{18}F]DOPA; [^{18}F]FP-CIT; [^{11}C]raclopride; [^{11}C]DTBZ; [^{18}F] β-CFT; [^{11}C]SCH-23390
	Cholinergic system	[^{123}I]A-85380	[^{18}F]FP-TZTP; [^{11}C]nicotine; [^{11}C]MP4A; [^{11}C]PMP; [^{8}F]A-85380
	Serotonergic system	[^{123}I]ADAM	[^{18}F]MPPF; [^{18}F]altanserin [^{18}F]setoperone; [^{11}C]DASP
	GABAergic system	[^{123}I]iomazenil	[^{18}F/^{11}C]flumazenil
	Opioid system		[^{11}C]carfentanil; [^{18}F]ciclofoxy
Biomarkers of dementia	Aβ deposits		[^{18}F]AV-45; [^{11}C]SB-13; [^{11}C]PiB; [^{18}F]BAY-94-9172; [^{11}C]AZD-2184
	τ protein		[^{18}F]FDDNP
	Microglia		[^{11}C]PK11195; [^{11}C]DAA1106
	Astrocytes		[^{11}C]DED

Regarding PET imaging, [^{15}O]H_2O can be considered the brain perfusion agent *par excellence* because its retention time and clearance are directly proportional to blood flow in a given tissue, independently of its metabolism and possible pathophysiological changes[42]. [^{18}F]FDG studies of cerebral glucose metabolism, which allow inferences

about synaptic activity, has shown great importance in the separation of the various dementias since the cognitive and functional changes, and consequently the brain regions affected, are different[43, 44]. The cases of patients with AD normally demonstrated a classical pattern of bilateral glucose hypometabolism in the parieto-temporal lobes, which does not happen in most other dementias[45].

Looking at Table 2.1 it is clear that as the biological processes under study become more specific the availability of SPECT tracers diminishes. This is due to the fact that their chemistry is essentially based on complexes of transition and post-transition metals with high atomic number and no relevance in living systems, making them highly reactive and bioaccumulable. It is, therefore, difficult to synthesize radiotracers with high specificity for biological processes at a nano or picomolar scale. One attempt to solve this problem is through the use of iodine radioisotopes since they can be easily introduced on the tyrosine, histidine or histamine residues although, on the other hand, they also have the disadvantage of being able to cause a significant increase on the lipophilicity of the biomolecules[33, 46]. Therefore, the alternative is to use PET radiotracers that can be labelled with radioisotopes from the most prevalent elements in organic molecules which allow the labelling of, virtually, any molecule without losing its biological activity. The development of PET technology associated with the availability of different radiotracers increased the sensitivity in clinical evaluation and differentiation of dementias (see Figure 2.2). Up to this point dementias were often erroneously confused with normal cognitive decline inherent to aging and failures in its diagnosis reached values in the order of 40% to 90%[47]. In parallel to the technological advances of the radiation detection systems and to the development of new hybrid systems, in particular PET/MRI that adds a high spatial resolution technique (MRI) to the high sensitivity of PET, the ability to synthesized radiotracers with increasing specificity for the characteristic molecular targets of each dementia made possible a more assertive diagnostic.

Cholinergic receptors and amyloid plaques are, as mentioned above, two of the major molecular targets in Alzheimer's disease so there has been a growing interest in the synthesis of biospecific radiotracers to target them. Studies with [^{11}C]nicotine and [^{18}F]A-85380 mapped nicotinic cholinergic receptors of neuroglia and concluded that their levels are dramatically reduced in patients with AD[48, 49]. Another way to study indirectly the cholinergic receptors is by the acetylcholinesterase activity as this enzyme is responsible for the degradation of acetylcholine in the cerebral cortex. If cholinergic receptors are reduced in AD then it is expected that the neurotransmitter

acetylcholine is also diminished, which means a decline in the acetylcholinesterase activity such as revealed by studies with [^{11}C]PMP and [^{11}C]MP4A[5, 50].

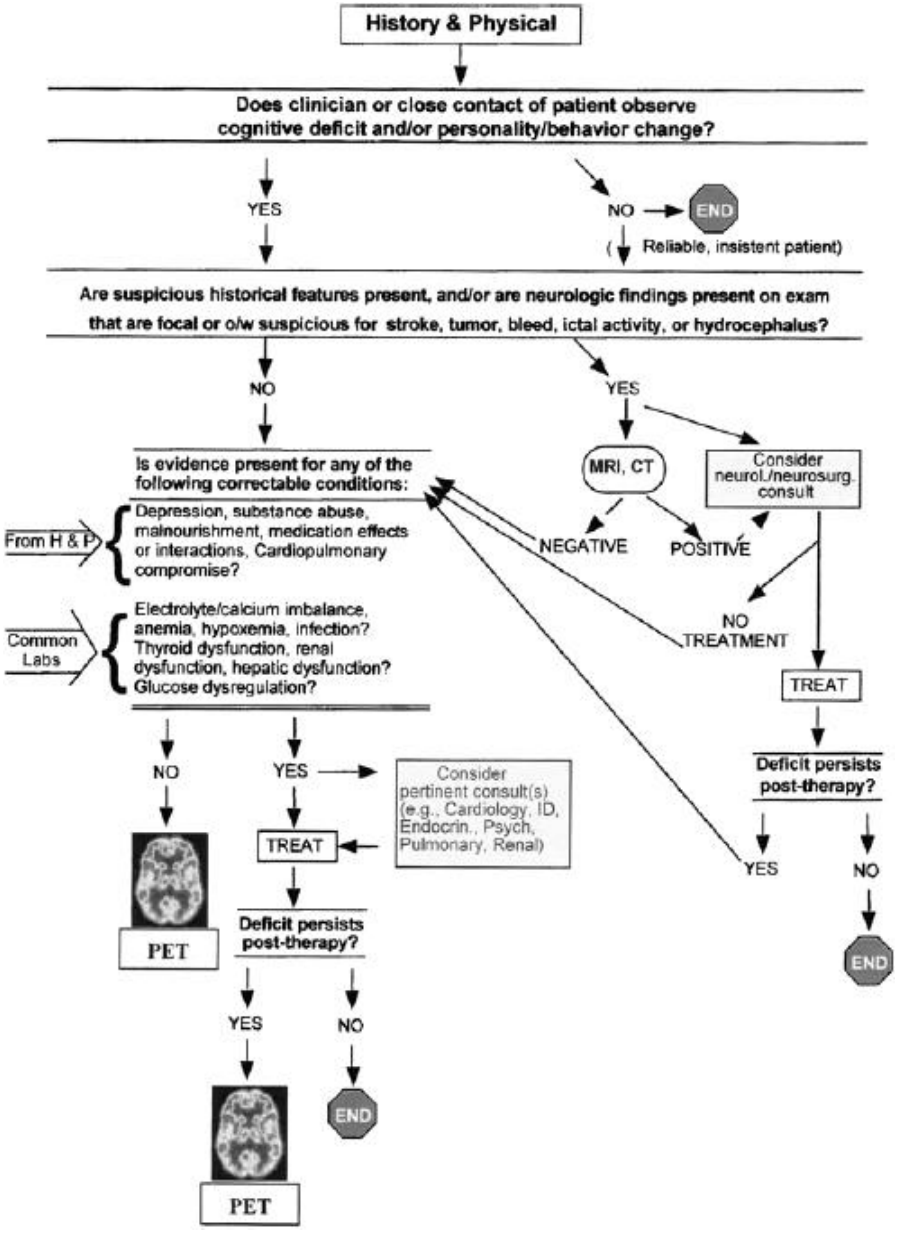

Figure 2.2. Flow chart for evaluation of PET brain studies. (Silverman[51])

[^{18}F]FDDNP was the first PET radiotracer that allowed *in vivo* imaging of AD by binding to τ proteins in neurofibrillary tangles[52]. Despite the difficulties in synthesizing radiotracers with affinity for the amyloid plaque mostly due to ignorance of all AD mechanisms, some molecules such as [^{11}C]SB-13 and [^{11}C]PK11195 were synthesized

later and proved to be clinically interesting and helped to better understand the stages of amyloid cascade[30, 53]. However, it was only with the development of [^{11}C]PiB, a benzothiazole derived from thioflavin T that binds *in vivo* to Aβ deposits in a manner that is strongly correlated with the amount of Aβ deposits observed post-mortem in brain tissue of AD patients, that became possible to realize PET quantification studies of senile plaques[54-57]. Although having the disadvantage of the short half-life of ^{11}C that prevents its distribution to Molecular Imaging centres without a cyclotron, [^{11}C]PiB is now well established in the literature as the reference radiotracer for AD due to its high sensitivity (89%) and very good specificity (83%) for earlier detection of the disease[58-61]. The exact way by which [^{11}C]PiB binds to the Aβ plaques is not completely understood but *in vitro* studies showed specific binding only to extracellular and intravascular deposits of Aβ oligomers and not to the unbound and free peptides[54, 57, 62]. Intravenous (i.v.) administration of low nanomolar concentrations is enough to obtain a satisfactory biodistribution of the radiotracer in order to have sufficient affinity for the Aβ plaques without binding to other aggregates such as neurofibrillary tangles or α-synuclein and ubiquitin in Lewy bodies dementia, while maintaining a rapid clearance of normal brain tissue[56, 63, 64]. This has consolidated [^{11}C]PiB as not only the gold standard for *in vivo* quantification of Aβ deposits in PET diagnosis of AD but also as an important tool to establish the relationship between Aβ affected areas and functional or structural changes which enables, for example, an appropriate selection of patients for new anti-amyloid therapies[64].

The pharmaceutical industry has estimated a potential market of around 500 million dollars a year, in the coming decades, for biomarkers and molecular probes designed for the diagnosis of AD. There are already some fluorine-18 based radiotracers in phases II and III of clinical trials or in the process of market authorization such as 3'-[^{18}F]-PiB (*GE Healthcare*), [^{18}F]BAY-94-9172 (*Bayer*) and [^{18}F]AV-45 (*Lilly pharmaceutical*) which have proved to be promising in the differentiation of patients with AD[58, 65]. However [^{11}C]PiB still remains the benchmark for the development of these new tracers.

2.2.1 [^{11}C]PiB in the differentiation of Alzheimer's disease

By having a high affinity for Aβ deposits (K_d = 1.4 nM), easy access through the BBB and low toxicity, [^{11}C]PiB is currently the radiotracer with greater specificity and sensitivity for early detection of Aβ plaques and vascular amyloid deposits in the

brain[54, 66]. A brain protocol for studies with [^{11}C]PiB must respect the same general contraindications and previous preparation of the patient that routine scans with [^{18}F]FDG[67]. Even if brain uptake of [^{11}C]PiB is not dependent on the surrounding conditions it should always be taken into account patient rest in a controlled, comfortable and quiet environment and the use of anaesthetics or sedatives equated only in extreme cases[68]. In patients with suspected AD a prominent uptake of [^{11}C]PiB is expected in frontal and parietal lobes and a reduction in temporal lobes[56]. [^{11}C]PiB has a non-specific affinity for the cerebral white matter which has been attributed to a decrease of the radiotracer kinetic in this region[69]. However its effectiveness in diagnosis of AD is approximately 90%[70] and the cerebral retention rate about two times higher than in normal patients[71].

Longitudinal studies have shown that the pattern of brain uptake of [^{18}F]FDG and [^{11}C]PiB differs over time and that the amyloid deposits appear to occur before cognitive symptoms and, perhaps, even before there were a minimum impairment of memory[72]. This way it can be possible to discriminate, through [^{11}C]PiB studies, different stages of AD according to Aβ deposits localization and concentration within the cerebral cortex[73] (see Figure 2.3). The possibility of Aβ deposits quantification through [^{11}C]PiB brain uptake is a major advantage that can be used to differentiate patients with AD or mild cognitive impairment (MCI) from healthy subjects (see Figure 2.3)[51, 64, 66, 74, 75]. The uptake pattern of [^{11}C]PiB in a PET scan also demonstrated some potential in differentiating between AD and Lewy bodies dementia, frontotemporal dementia and Parkinson's, having this last one, an amplification of the radiotracer retention in the mesencephalon[30].

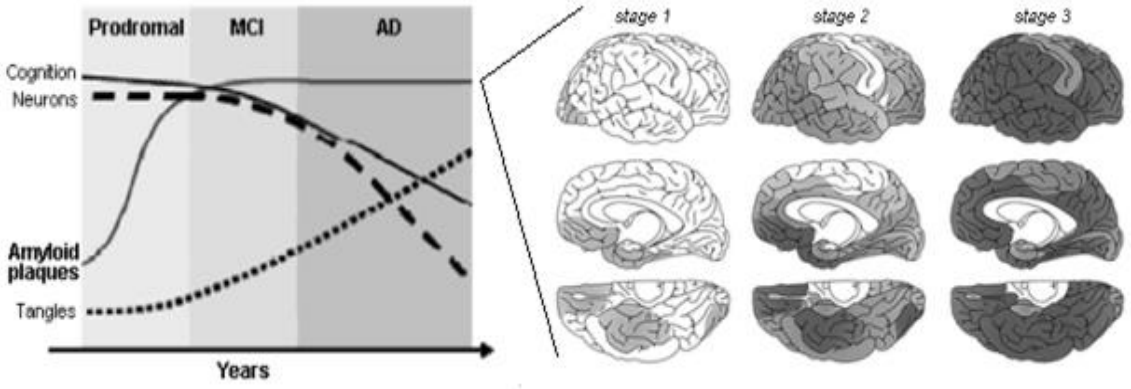

Figure 2.3. Progression of Aβ deposits in AD. (Adapted from Nordberg[73] and Langstrom[75])

Comparative PET scans in patients with MCI, that due to its progression rate for AD of 80% in 6 years is considered the ideal etiological stage to evaluate an early diagnosis of AD, found that [^{11}C]PiB has greater sensitivity and specificity than [^{18}F]FDG in anticipating ongoing brain function atrophy[76, 77].

2.3 Synthesis of short lived PET radiotracers

Fluorine-18 (^{18}F), carbon-11 (^{11}C), nitrogen-13 (^{13}N) and oxygen-15 (^{15}O) are the most frequently used radionuclides in PET (see Table 2.2). This is, in part, due to the fact that they can be produced efficiently in a medical cyclotron and have a radioactive decay almost exclusively by β^+ emission but especially because they are isotopes of elements with low atomic mass that are highly prevalent in all organic molecules. This makes them easy to introduce directly in any molecule of interest without modifying significantly its biological activity. The production of radioisotopes requires the existence of a particle accelerator capable to generate proton or deuteron beams with sufficient energy that can be directed to a specific target material suitable for the production of ^{11}C, ^{13}N, ^{15}O, ^{18}F or other.

Table 2.2. Features of most commonly used PET radionuclides[78]

Radionuclide	$t_{1/2}$ (minutes)	Nuclear reaction	Target	Primary precursors	Decay product
^{15}O	2.04	^{14}N(*d,n*)^{15}O	N_2(+O_2)	[^{15}O]O_2	^{15}N
^{13}N	9,97	^{16}O(*p, α*)^{13}N	H_2O H_2O+EtOH	[^{13}N]$NO_{2/3}$ [^{13}N]NH_3	^{13}C
^{11}C	20.4	^{14}N(*p,α*)^{11}C	N_2(+O_2) N_2(+H_2)	[^{11}C]CO_2 [^{11}C]CH_4	^{11}B
^{18}F	109.8	^{20}Ne(*d,α*)^{18}F ^{18}O(*p,n*)^{18}F	Ne(+F2) [^{18}O]H_2O	[^{18}F]F_2 [^{18}F]F^-	^{18}O

The interest in these positron emitters increased in the 1970s when technological advances allowed the detection, in coincidence, of both γ photons that arise from the emission process enabling the production of images capable of reveal molecular

processes and interactions *in vivo*[79]. These photons result from the annihilation of positrons (β^+ particles) with electrons at the surrounding tissue generating two detectable anti-parallel 511 keV γ rays. The critical parameter regarding this radionuclides are their short half-lives ($t_{1/2}$), which means that production, synthesis, quality control and imaging must be time compatible with this physical property (see Figure 2.4). Due to the favourable $t_{1/2}$, the only commercially available compounds are radiolabelled with ^{18}F while the use of the other radionuclides is limited to facilities where cyclotron, radiochemistry labs and appropriate diagnostic equipment coexist[38].

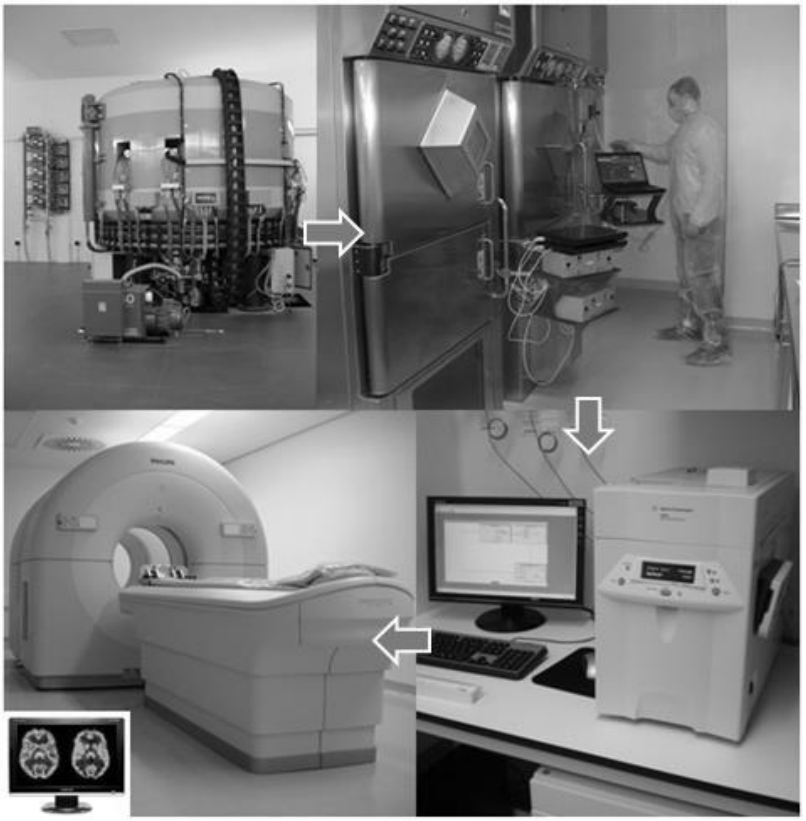

Figure 2.4. Pathway from cyclotron production to final use of a PET tracer.

The synthesis of all PET radiotracers begins from simple primary radioactive precursors resulting from reactions that occur in the particular environment of the cyclotron target between high energy particle beams (usually protons and neutrons) and selected stable nuclei. In these favourable conditions it is possible to overcome the barrier of activation energy and produce, by a nuclear reaction, unstable nuclides in a chemical form that is frequently determined by the thermodynamics of each constituent,

which leads to very stable and unreactive molecules[79]. From these primary precursors is often necessary to quickly synthesize other secondary ones with greater reactivity and which can be introduced, as late as possible, into more complex molecules, a process that is often followed by a purification step in order to isolate the final product. Radiolabelling reactions occur in the presence of nanomolar quantities of the radioisotope which means that there is a stoichiometric excess of the cold reagents. This promotes first order reactions kinetics and reduces the total synthesis time[78].

The development of automatic and remotely controlled procedures for handling radioisotopes and the improvement of radiochemistry is essential to ensure maximum radiological protection and reproducibility, especially in cases where these procedures are routinely performed for clinical applications.

The short $t_{1/2}$ of ^{13}N and ^{15}O does not allow synthesis with more than one step that typically requires time-consuming purification methods, so their application is usually limited to the incorporation into small molecules. Simpler chemical forms such as $[^{15}O]CO_2$, $[^{15}O]H_2O$ and $[^{13}N]NH_3$ can be directly obtained from cyclotron and used in blood flow studies or be quickly converted into other products such as $[^{15}O]CO$, $[^{15}O]$*n*-butanol or $[^{13}N]$cisplatin[78]. The enzymatic synthesis of $[^{13}N]$amino acids with high yield and purity and without loss of biochemical activity, is one of the most frequently used approaches to these radionuclides and allows, for example, the study of cellular proliferation or the evaluation of cardiac metabolism[80].

Despite not being a common element in the structure of biomolecules, the proximity of Van der Waals radius with the one of atomic hydrogen, their similar covalent bond length with C and a convenient $t_{1/2}$, made fluorine-18 the most widely used PET radionuclide[81]. The chosen nuclear reaction in the cyclotron affects the chemical form ($[^{18}F]F_2$ or $[^{18}F]F^-$) and the nature (electrophilic or nucleophilic) of the obtained ^{18}F which increases the possibility of radiofluorination of different molecules of interest. The electrophilic substitution allows the easy insertion of the radioactive fluorine in electronically rich structures (aromatic rings or alkenes) but, due to its high reactivity, reactions are not regioselective leading to a lower radiolabelling yield which requires a more complex chromatographic separation. This reactivity may be moderated by dilution with an inert gas and working at low temperatures but the reaction will always lead to products with low SA due to the production method of $[^{18}F]F_2$ that requires the addition of a small amount of cold fluorine (carrier) to prevent adsorption to the target. For avoiding these drawbacks, the nucleophilic substitution using $[^{18}F]F^-$ is a preferable

and most common method for the preparation of the majority of PET radiotracers although, in some cases, it is necessary the introduction of prosthetic groups and the protection of more reactive positions in the target molecule[78].

The introduction of a foreign element in the original chemical structure of a molecule, as often happens in the case of fluorination, may cause a change in biological properties. The presence of carbon atoms in all relevant biomolecules makes the radiolabelling with ^{11}C the most attractive (except in molecules with long term biodistribution, e.g., proteins) and important method for the synthesis of PET radiotracers since it offers the possibility of labelling molecules without changing its chemical and biological characteristics. This factor is especially important in compounds for brain studies as the preservation of physicochemical characteristics is essential for the BBB permeability and for the affinity to specific molecular targets.

With a $t_{1/2}$ of approximately 20 minutes, the major challenge in the use of ^{11}C is the development of increasingly fast, reliable, versatile and automated radiosynthesis procedures starting from the less reactive primary precursors $[^{11}C]CO_2$ or $[^{11}C]CH_4$.

2.3.1. Carbon-11 radiochemistry

The carbon atom is a transversal constituent of all biological molecules. For this reason, and due to the relative ease with which it can be incorporated into biomolecules of interest without significant loss of chemical properties and biological activity, ^{11}C is one of the most commonly used radioisotopes in the synthesis of radiotracers. However, side reactions with atmospheric $[^{12}C]CO_2$ and a half-life of about 20 minutes make the synthesis of ^{11}C radiotracers with high SA a real challenge in radiochemistry. So, despite the fact that virtually all potentially interesting biomolecules can be labelled with ^{11}C, this is far from being a linear process.

Radiochemical reactions should occur as quickly as possible (typically a maximum of 5 minutes) and present reasonable yields and low quantities of side products, so that the final product can be rapidly purified, usually by HPLC. The resulting radiotracer should have high chemical and radiochemical purity and has to be formulated to produce a sterile non-pyrogenic solution ready for i.v. administration. The whole process should not exceed the time corresponding to two ^{11}C half-lives, i.e., approximately 40 minutes. Precursors for the most common ^{11}C radiotracers are

commercially available and an intense activity of research has developed a wide variety of reactions for their radiolabelling[81].

The production of ^{11}C is made by cyclotron irradiation of a nitrogen gaseous target with protons according to the nuclear reaction $^{14}N(p,\alpha)^{11}C$. Depending on whether the irradiation is carried out in the presence of O_2 (0.5-1%) or H_2 (5-10%), ^{11}C is obtained in the chemical form of $[^{11}C]CO_2$ or $[^{11}C]CH_4$ which, being species with low reactivity, require the synthesis of other more reactive (secondary) precursors (see Figure 2.5).

The development of strategies for labelling with ^{11}C using, for example, reactions with phosgene ($[^{11}C]COCl_2$), cyanide ($[^{11}C]HCN$), carbon dioxide ($[^{11}C]CO_2$) and carbonyl ($[^{11}C]CO$) increased the diversity of molecules containing this radionuclide that can be synthesized[82]. However, $[^{11}C]CH_3I$ is the most widely used secondary precursor since it is more versatile in alkylation reactions and it also has the advantage of being synthesized by different pathways.

The synthesis by the so called “gas phase method” starts with $[^{11}C]CH_4$, obtained either directly from the cyclotron or by reducing $[^{11}C]CO_2$ through nickel catalysis. $[^{11}C]CH_4$ is then converted in $[^{11}C]CH_3I$ in the presence of iodine vapours at elevated temperature (approx. 700° C)[83]. This pathway provides clear advantages for not using aggressive reagents and leads to higher SA of the final product (due to the low amount of $[^{12}C]CH_4$ in the air, approximately 1.6 ppm, in contrast to the 330 ppm of $[^{12}C]CO_2$). Nevertheless, the greater ease of automation of the $[^{11}C]CH_3I$ synthesis by the “wet method” with very efficient final yields, leading to bigger absolute quantities of ^{11}C, makes this technique the most commonly used[82].

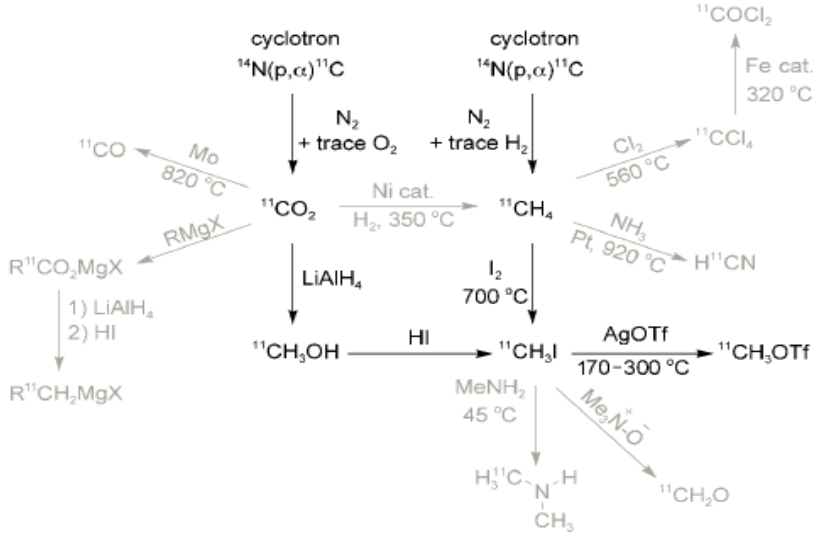

Figure 2.5. Radioactive precursors for ^{11}C synthesis. (Adapted from Scott[84])

In the synthesis of [^{11}C]CH_3I by the “wet method”, [^{11}C]CO_2 is reduced to [^{11}C]methanol ([^{11}C]CH_3OH) in the presence of lithium aluminium tetrahydride ($LiAlH_4$) in tetrahydrofuran (THF). After THF evaporation a hydrolysis by hydriodic acid (HI) is carried out followed by a distillation of the [^{11}C]CH_3I. All this process should occur in an inert atmosphere and under anhydrous nitrogen or helium flow in order to avoid [^{12}C]CO_2 in the reaction environment. In fact, contamination with atmospheric CO_2 is the main problem in this method as it is also reduced with $LiAlH_4$ (in competition with [^{11}C]CO_2) and will cause a dramatic reduction in the specific activity of [^{11}C]CH_3I and, consequently, of the final alkylation product.

Due to its simplicity, speed and to the fact that many biomolecules contain a methylamine, aniline or anisole pharmacophore, the most commonly pathway of methylation with ^{11}C is by SN_2 nucleophilic substitution. This reaction occurs from previously demethylated compounds containing primary amines, thiol or hydroxyl groups and, in many cases, require the presence of a base for catalyzing its deprotonation[82]. The understanding of the metabolism of a radiotracer is also essential for a successful synthesis since there are frequently several positions in the molecule that can be labelled with the radioisotope. Ideally, active metabolites containing the radioisotope should not be formed, as they can mask the signal of the main radiotracer. PET radiotracers for the study of brain biochemistry are usually radiolabelled in a metabolically unstable position (e.g., a *N*-[^{11}C]CH_3 group) that, after administration, gives hydrophilic intermediate products, unable to cross BBB, which causes the brain signal externally detected to be exclusively related to the intact radiotracer[78].

Some radiotracers have low radiochemical yields when labelled with [^{11}C]CH_3I. In these cases the methylation agent [^{11}C]CH_3OTf, a more reactive and less volatile species, has some advantages such as the fact that the reaction can occur at room temperature with smaller amounts of precursor and shorter reaction times, which results in higher radiolabelling yields[85, 86]. The synthesis of [^{11}C]CH_3OTf is performed by passing [^{11}C]CH_3I in a nitrogen flow through a column filled with graphite and silver triflate preheated to 170° - 200° C[87].

Methylation by the captive solvent method has been the most used technique in the preparation of ^{11}C radiotracers due to the ease of automating of this procedure[88]. Here, the methylation agent [^{11}C]CH_3I or [^{11}C]CH_3OTf is trapped into a solid support, such as an HPLC loop or a solid phase extraction column (SPE), containing a solution with micromolar amounts of the chemical precursor dissolved in a polar aprotic solvent,

usually dimethyl sulfoxide (DMSO), dimethylformamide (DMF), acetonitrile (CH_3CN), methyl ethyl ketone (MEK) or another ketone[80]. This kind of solvents does not form hydrogen bonds with the nucleophiles, so will not suffer a loss of reactivity, and will have the ability to trap the methylation agent stabilizing the leaving group.

Reactions that occur directly in a loop system associated to an HPLC and previously coated with chemical precursor solution allow a simplified experimental setup, easily automated and without significant loss of activity during the transfer to the chromatographic system (see Figure 2.6). Other advantages result from the fact that loop geometry allows the reduction of the volume of solvent used, increasing the concentration of the chemical precursor, which leads to faster reactions at room temperature and better yields[89].

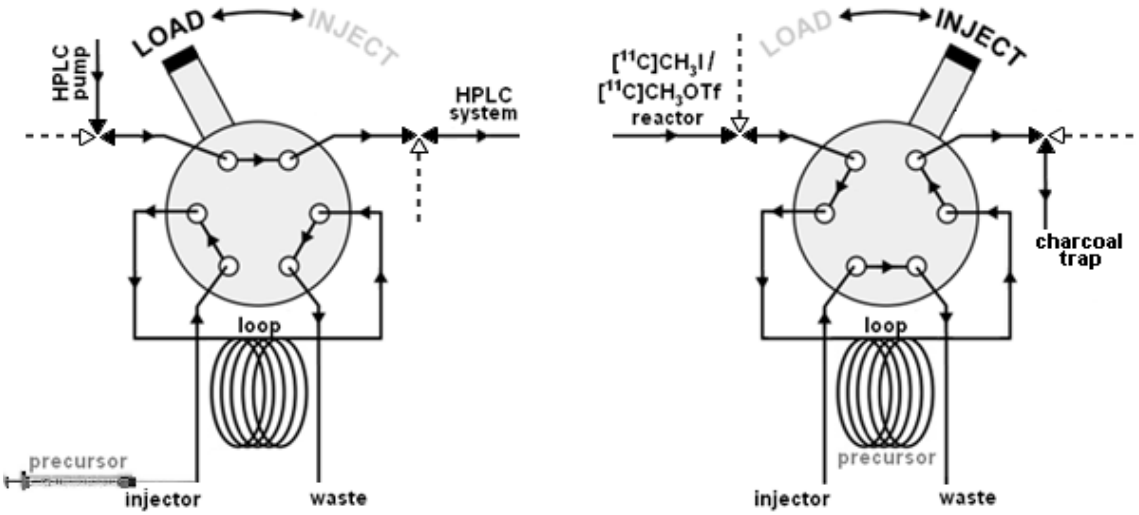

Figure 2.6. Scheme of loop injector as a solid phase reaction system.

In the last decade several ^{11}C-labelled radiotracers have been synthesized using different methylation approaches. The indirect method using [^{11}C]dimethylamine, and starting from brominated precursors, is an interesting alternative in the alkylation of compounds with dimethylamine functional groups in their structure[90]. Also palladium-mediated methylations with [^{11}C]CH_3I either by Stille (which starts with tin-activated precursors) or Suzuki (which starts with organoboron precursors) coupling reactions have demonstrated particular interest especially because of the inherent

advantage to facilitate the chromatographic separation of the labelled final product[80, 91].

Similar to the optimization of reaction conditions, the development of a chromatographic method that enables an efficient separation of the radiotracer from the precursor and other secondary products is an important problem to solve in the radiosynthesis with ^{11}C. However, the major challenge lies in the strict need to exclude from the system possible sources of contamination with humidity and atmospheric stable carbon that are the main causes to the critical reduction of the SA of the radiotracer.

Specific activity is defined as the fraction of the radiotracer, expressed in units of Becquerel or Curie (Bq or Ci), in relation to the total number, both radioactive and stable, of molecules of that same species. This property is particularly relevant in PET radiotracers specifically directed to molecular targets easily saturable (e.g., receptors or antigens) and whose density is sometimes limited by the anatomical structures in study. Although Aβ plaque is not a brain receptor, the mechanism of its imaging is the same as that of other receptor agents. For this reason, and particularly in brain imaging, the coexistence of the tracer both labelled with ^{11}C and stable ^{12}C may lead to pharmacodynamic or toxic undesirable effects, as well as distorted results of the processes in study, due to the competitive blocking of the molecular targets with the cold compound.

Synthesis of ^{11}C radiotracers is nowadays performed in automated synthesis modules. This brings obvious advantages regarding radiation protection, reproducibility and efficiency in the radiosynthesis. Nevertheless, the procedure is far from being routine and for each production centre and for each radiotracer a process optimization procedure must be developed in order to obtain a final product that meets all pharmaceutical requirements for human use.

2.3.2 Pittsburgh Compound B radiosynthesis

In the late 1990s thioflavin T, a benzothiazole (BTA) that has a characteristic red fluorescence emission when it binds to β-sheet structures, proved to be useful in the histological analysis and quantification of amyloid aggregates[92]. However, the evidence that the cationic nature of this compound hinders its passage through BBB has led Mathis and Klunk research group, in the year 2000 at the University of

Pittsburgh, to the synthesis of a neutral and lipophilic analogue [*N*-methyl-^{11}C]2-(4'-(methylaminophenyl)-6-methylbenzothiazole ([^{11}C]6-Me-BTA-1) that showed better pharmacokinetic and a higher affinity for the Aβ deposits[93] (see Figure 2.7). The persistence on improving the characteristics of this molecule culminated in the synthesis of the promising so-called Pittsburgh Compound A ([*N*-methyl-^{11}C]2-(4'-(methylaminophenyl)-benzothiazole or [^{11}C]BTA-1) with improved cerebral uptake[94] and then the currently known as Pittsburgh Compound B ([*N*-methyl-^{11}C]2-(4'-(methylaminophenyl)-6-hidroxibenzothiazole, [^{11}C]6-OH-BTA-1 or [^{11}C]PiB)[95]. Although the early studies have focused mainly in [^{11}C]BTA-1, subsequent *in vitro* and *in vivo* results have shown that although [^{11}C]PiB does not present an initial high brain uptake it has, however, a lower non-specific binding, a greater regional homogeneity and a faster clearance from the non-pathological brain which improves the cerebral uptake ratio between individuals with and without AD[96]. Currently there is a consensus that [^{11}C]PiB is the leading PET radiotracer for the early diagnosis of Aβ deposits which makes it a very valuable tool for centres that meet the peculiar and necessary conditions for its synthesis and use[51].

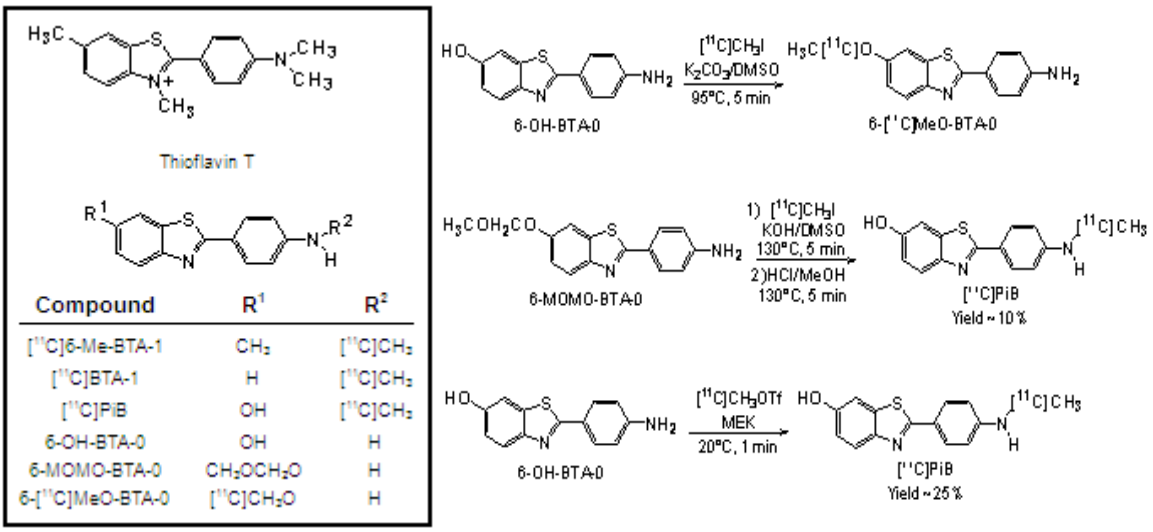

Compound	R^1	R^2
[^{11}C]6-Me-BTA-1	CH_3	[^{11}C]CH_3
[^{11}C]BTA-1	H	[^{11}C]CH_3
[^{11}C]PiB	OH	[^{11}C]CH_3
6-OH-BTA-0	OH	H
6-MOMO-BTA-0	CH_2OCH_2O	H
6-[^{11}C]MeO-BTA-0	[^{11}C]CH_2O	H

Figure 2.7. Structure of thioflavin T analogues and radiolabelling reactions.

The main chemical precursor for the synthesis of [^{11}C]PiB is 2-(4'(aminophenyl)-6-hidroxibenzothiazole (6-OH-BTA-0) synthesized from the processing of 4-methoxy-phenylamine into the corresponding nitrothiobenzamide with

subsequent cyclization, reduction of nitro functional group and demethylation[96]. First attempts to the direct methylation of this precursor with [^{11}C]CH_3I showed a higher reactivity of the hydroxyl group and that the desirable [^{11}C]N-methylation was not detectable, which originated a radiotracer with uninteresting pharmacokinetics (6-[^{11}C]MeO-BTA-0). Protection of the phenol with a methoxymethyl group (6-MOMO-BTA-0) has favoured the nucleophilic substitution in the primary amine but requires an additional deprotection step which increases the reaction time, the need of more aggressive conditions and the use of more refined purification techniques to obtain [^{11}C]PiB in a final saline solution suitable for i.v. administration[96] (see Figure 2.7).

Using [^{11}C]CH_3OTf as a direct methylation agent of the desmethyl precursor 6-OH-BTA-0 by a loop captive solvent method, Wilson and his co-workers have developed a more efficient radiolabelling methodology of [^{11}C]PiB which only causes secondarily a vestigial amount of [^{11}C]MeO-BTA-0 easily separated from the final solution by HPLC[97] (see Figure 2.7). Considering that [^{11}C]CH_3OTf is more reactive and less volatile than [^{11}C]CH_3I, its methylations can occur without the use of forced conditions - which often promote the formation of side products that must be removed - and can be easily trapped and confined into limited geometries, such as a loop system[87].

With the commercial availability of the precursor 6-OH-BTA-0, this last method has become the main route for the preparation of [^{11}C]PiB and, since then, several authors[97-102] have automated and optimized it for their particular laboratory realities, which means that there is no consensus on what are the more suitable reaction conditions (temperature, time of reaction, solvent and precursor concentration) since these ultimately depends on the particularities of each synthesis system assembled. That is why it is essential to optimize the whole process of [^{11}C]PiB synthesis when it is originally implemented in a research or diagnostic centre.

3. Justification of the project

This scientific and technical work that support this thesis were performed at ICNAS with the aim of establishing an automated and reproducible process for radiolabelling of [^{11}C]PiB, through the captive solvent method, and further purification and reformulation in a sterile and pyrogen-free injectable solution. The goal was to produce a sterile apyrogenic injectable solution of [^{11}C]PiB with good yields, high purity and adequate SA for human studies.

Since the academic degree involved has a main objective of providing vocational qualifications and skills that aim to contribute to an improvement of healthcare, we consider that this project totally fulfils that purpose.

The fact that the synthesis of [^{11}C]PiB is described in the literature does not affect the importance of this project as its radiolabelling, purification, and reformulation in a sterile non-pyrogenic injectable are new in Portugal and need to be adapted for local applicable regulations. Moreover, this process is not fully described when using the sequential line of the automated modules MeI-Plus^{TM}, AutoLoop^{TM} and ReFORM-Plus^{TM} (Bioscan Inc. Washington DC, USA) and several parameters need to be optimized for a successful, reliable and reproducible synthesis. Conversely, the existence of vast scientific evidences that confirm the technical importance of [^{11}C]PiB-PET/CT in early clinical diagnosis of AD reinforces the need of its availability to the population in face of a health problem with such great impact on contemporary societies.

In a radiopharmacy expertise degree that aims primarily to provide Nuclear Medicine students with important qualifications for their professional life (taking into account the available resources and the labour market demands due to the technological and scientific evolution) we consider very pertinent to chose the optimization of an already known radiotracer with real impact on the clinical practice rather than investing all efforts in new chemical entities developed with investigational purposes that, many times, have more in mind to advance the radiochemistry science than to respond to real needs of the clinical practice. These results, despite giving origin to dissertations of undeniable interest, typically are too centred on the theories and techniques which deflect them from what should be their true assumption: to assist with actually relevant

radiopharmaceuticals, that meet the needs of clinical molecular imaging, in order to have a real impact on populations and healthcare systems.

Considering that the proposed project involved highly specific equipment, complex chemical reagents and short-lived radionuclides, it was essential to use a radionuclide production facility containing a cyclotron and a radiochemistry laboratory with the automated synthesis modules and all other devices and materials needed for the realization of such a work. Bearing in mind the costs involved, the project was subjected to scientific and economical evaluation by ICNAS and it was considered very relevant taking into account the objectives of the centre, as laid down by its scientific council, and also economically viable considering the potential for human studies. The interest of ICNAS in the results was crucial for the development of the work and corroborates the relevance and appropriateness of this project.

The work was conducted under Good Laboratory Practices (GLP), Good Manufacturing Practices (GMP) and current Good Radiopharmacy Practices. (cGRPP). Research with this compound was submitted to the University of Coimbra ethics committee for human use and approved for clinical studies. This entity falls within the responsibility of the Portuguese *Decreto-Lei nº 97/95* of May 10th and *Lei nº 46/2004* of August 19th, according to *Artigo 12º* from *Regulamento Interno do ICNAS*, to certify the execution of ethical standards in the exercise of medical sciences, in order to protect and ensure human dignity and integrity, by conducting an analysis and reflection on issues of clinical practices that may involve an ethical discussion.

4. Methodology

The preparation of the radiotracer was based on the captive solvent method developed by Wilson and co-workers[97]. The processes of radiolabelling, purification and reformulation of [^{11}C]PiB were automated in order to obtain a sterile, non-pyrogenic, injectable solution to carry out PET research studies. Starting from [^{11}C]CO_2 produced in a Cyclone® 18/9 cyclotron (IBA©, Louvain-La-Neuve, Belgium) by the $^{14}N(p,\alpha)^{11}C$ nuclear reaction in a N_2 + 0.5% O_2 gaseous target, the synthesis of the radioactive precursor [^{11}C]CH_3I and then [^{11}C]CH_3OTf by the "wet method" was optimized, using the MeI-Plus™ module. By reacting, at room temperature, in the AutoLoop™ system, the produced [^{11}C]CH_3OTf and the commercially available demethylated precursor 6-OH-BTA-0 under various conditions (time, solvent, concentration) the most favourable results for the [^{11}C]PiB production were determined and its quality, after reformulation in the ReFORM-Plus™ module, was confirmed through previously optimized analytical methods (see Figure 4.1).

The radiosynthesis was carried out in a hot cell with the operator making exclusive use of remotely controlled equipment, manipulators and valves whilst visually monitoring all the process through a leaded-glass window and by a software program that gives a graphical view of each operation and monitored function (flow, pressure, temperature and radioactivity). In-process controls provided the evidence of the intermediate and final results and were collected and recorded throughout the course of the procedure.

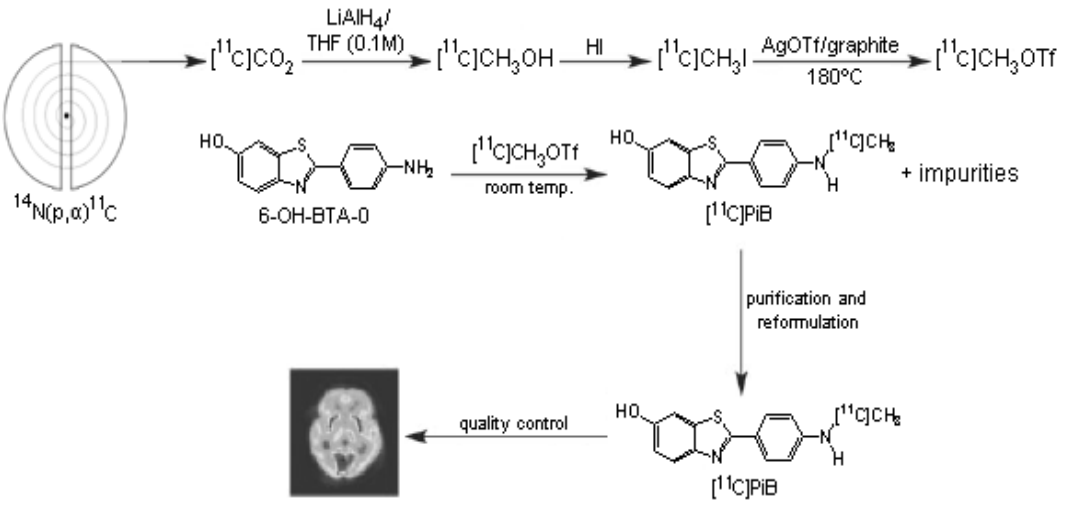

Figure 4.1. Scheme of the adopted [^{11}C]PiB synthesis process.

4.1 Instruments and materials

Apart from the Bioscan Inc. commercial modules previously described and IBA© cyclotron Cyclone® 18/9, several other specific and scientific devices were needed for this project (see Figure 4.2).

All radiochemistry procedures were carried out in a shielded MIP1-1P hot cell (Comecer SPA©, Castel Bolognese, Italy). The semi-preparative HPLC system, coupled in series with AutoLoop™, was composed by a Wellchrom HPLC-Pump K-501 and a K-200 WellChrom fixed ultraviolet (UV) wavelength (254 nm) detector (Knauer GmbH©, Berlin, Germany) equipped with a Luna C18(2), 5 µm, 10x250 mm (Phenomenex®, Torrance, USA).

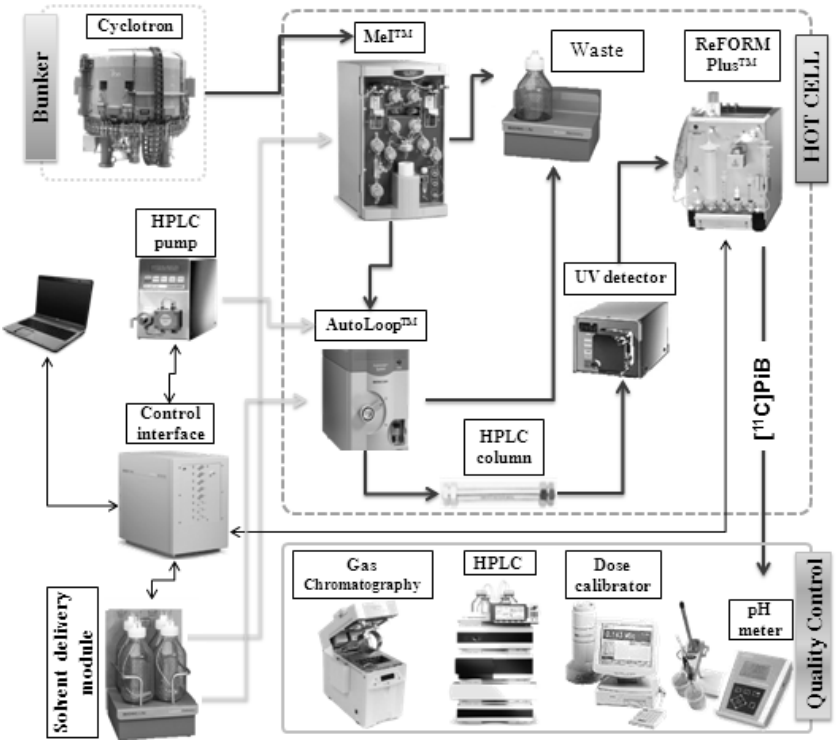

Figure 4.2. Diagram of the interactions between the devices involved.

Analytical equipment for quality control consisted of an Agilent 1200 Series HPLC UV system equipped with a Zorbax Eclipse XDB-C18 column, 5 µm, 4.6x150 mm (Agilent Technologies©, California, USA) and a GABIstar NaI(Tl) radiometric detector controlled via GINAstar software (Raytest Isotopenmessgeräte GmbH, Straubenhardt, Germany).

A Jenway 3510 pH meter (Bibby Scientific Limited©, Staffordshire, UK), an ISOMED 1010 dose calibrator (Nuklear-Medizintechnik Dresden GmbH, Dresden, Germany) and an Agilent 6850 Series II gas chromatography (GC) system with a HP-Fast GC Residual Solvent (6% Cyanopropylphenyl and 94% dimethylpolysiloxane, phase composition) capillary column (Agilent Technologies©) associated to a (FID), were also used.

The precursor 6-OH-BTA-0 (chemical purity >95%) and the cold PiB reference standard (6-OH-BTA-1) were obtained from ABX (ABX-Advanced Biochemical Compounds, Radeberg, Germany) while "cold" CH_3I was purchased from VWR® (VWR International SAS, Fontenay-sous-Bois, France). The reagents $LiAlH_4$ (0.1 M solution in dried THF) and HI (aqueous solution 57% redistilled over red phosphorus) were also obtained from ABX. Silver triflate, with trace metals basis upper than 99.95%, (Sigma-Aldrich®, Steinheim, Germany) and graphite powder (Bioscan Inc.) were used to prepare the column that converts $[^{11}C]CH_3I$ to $[^{11}C]CH_3OTf$. Molecular sieve adsorbent (13X, 100/120mesh), sodium hydroxide pellets (NaOH), phosphorus pentoxide (P_2O_5), CO_2 absorbent Ascarite II® (20-30 mesh) and ammonium formate (NH_4HCO_2) were purchased from Sigma-Aldrich®. Vented and 0.22 µm sterilization filter units (Millipore®, Carrigtwohill, Ireland) as well as three different kinds of C18 SPE cartridges (Waters®, Milford, USA) were used in the reformulation process.

All solvents were obtained from commercials suppliers at European Pharmacopoeia (Ph. Eur.), HPLC or *pro analysis* grade, as appropriate, and used without further purification while sterile water for injections (WFI) and 0.9% sodium chloride (NaCl 0.9%) were obtained from B. Braun© (B. Braun Melsungen AG, Melsungen, Germany). Pharmaceutical gases were purchased from Praxair© (Praxair Technology Inc., Danbury, USA) according to the composition and purity described in the Ph. Eur.

4.2 Experimental procedures

All of the procedures involving handling of radioactive substances were carried out in a radiochemistry laboratory with the standard required conditions of radiological protection and safety. The use of personal protective equipment and lead or tungsten barriers, with appropriate thickness to the manipulated activities, was equally transversal to all experimental procedures.

The adherence to GLP/GMP regulations, which deal with the organization, processes and conditions under which investigational studies should be planned, executed,

monitored and reported, became also essential to ensure that all data have been collected appropriately and that the inferred conclusions are valid. So, the date of receipt, quantity received, manufacturer, lot number, certificates and expiration date were recorded and archived for each of the components, materials reagents and supplies received and used.

4.2.1 Optimization of the chromatographic conditions

To optimize the chromatographic conditions for separation of PiB from the precursor 6-OH-BTA-0 and CH_3I it was carried out a bibliographic search of the HPLC eluent system and it was chosen the most appropriate flow for the used analytical (Zorbax Eclipse XDB-C18, 5 µm, 4.6x150 mm) and semi-preparative (Luna C18(2), 5 µm, 10x250 mm) columns.

The majority of the literature consulted mentions, as mobile phase of a reversed phase chromatographic system, an isocratic aqueous solution of 60% CH_3CN and 40% H_2O[97, 103-105] that, due to the presence of ionizable functional groups on the analyte, requires the addition of a buffer to adjust pH between 6.5 and 7.0. A 0.1 N ammonium formate buffer was used.

After selection of the chromatographic conditions that allowed a better performance in the separation of the analyzed compounds, these were identified by HPLC using commercially available reference standards and a calibration curve for subsequent quantification of PiB was built.

4.2.2 Production of $[^{11}C]CH_3I$ and $[^{11}C]CH_3OTf$

All PTFE and PEEK tubing as well as 3-way solenoid and 2-way pinched valves of MeI-Plus™ system were previously washed with ethanol, acetone and diethyl ether provided from solvent delivery module (see Figure 4.3). The $LiAlH_4$/THF and Hi reagent vials were also replaced by HCl 0.1 M and ethanol vials, respectively, to ensure the cleanliness of the dispensing valves, tubing and reactor. Finally all the system was carefully dried under a continuous nitrogen flow during at least 10 minutes, the $LiAlH_4$/THF and Hi reagent vials were then correctly placed in their corresponding positions and the module was pressurized to avoid external contamination.

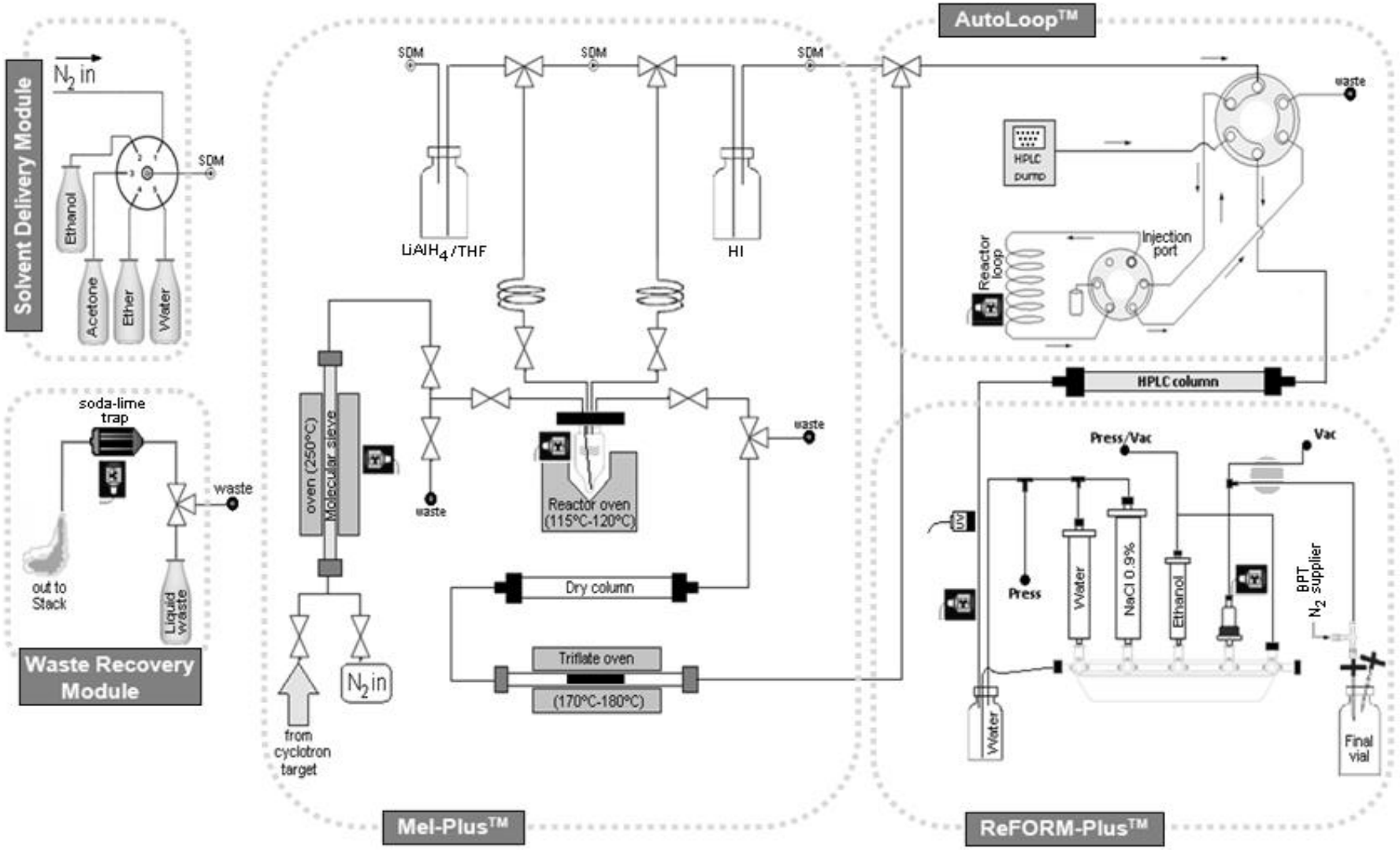

Figure 4.3. Schematic diagram of the automated ^{11C} radiolabelling system used.

Carbon-11 was initially produced in the form of $[^{11}C]CO_2$ at the cyclotron via the $^{14}N(p,\alpha)^{11}C$ in an aluminium body target loaded with N_2/0.5% O_2 gaseous mixture (purity above 99.99%) and covered with an aluminium window foil. The gas was irradiated with protons (effective beam energy on target of 16 MeV) with an integrated current between 10 to 14 µAh and the irradiation was stopped as soon as the desired activity level was reached. After cyclotron bombardment the $[^{11}C]CO_2$ was transferred by spontaneous expansion, through a stainless steel tube, to the synthesis module placed inside a hot cell in the radiochemistry laboratory. The radioactivity and its path along all the synthesis process can be monitored through several detectors strategically placed in the modules and hot-cell.

In a first step $[^{11}C]CO_2$ is trapped at room temperature in a copper column filled with molecular sieves (see Figure 4.4A). This column is previously conditioned by heating it at 250º C for at least 20 minutes and then cooled to remove traces of stable CO_2 which ensures a better SA. The reactor vessel is also prefilled with a given volume of $LiAlH_4$/THF. After the trapping of the $[^{11}C]CO_2$, the molecular sieve column oven is heated at 250º C under 12 ml/min continuous nitrogen flow during at least 1.5 minutes. This releases the $[^{11}C]CO_2$ from the column forcing it to bubble in the $LiAlH_4$/THF solution where is trapped in the reactor. Once the $[^{11}C]CO_2$ is completely trapped, THF is evaporated to dryness (>2 minutes at 115º-120º C) and an excess of HI (350-450 µl) is added to generate $[^{11}C]CH_3I$ which was then distilled under continuous nitrogen flow (3 minutes at 115º-120º C).

The volume of $LiAlH_4$/THF dispensed from the sealed vial was optimized to achieve a minimum amount capable of producing satisfactory conversion yields of $[^{11}C]CH_3I$. This is critical to SA, since atmospheric CO_2 is also trapped in the $LiAlH_4$/THF solution and the non-radioactive species derived from it are generated before the treatment with HI.

While other ^{11}C species go into waste, the distilled $[^{11}C]CH_3I$ passes with a nitrogen flow rate of around 12 ml/min through a 180º C preheated column filled with a not too much compressed mixture of graphite and silver triflate (see Figure 4.4B) to form $[^{11}C]CH_3OTf$. Since it is essential to ensure the homogeneity of this mixture it was produced by adding in a reaction flask 1 g of silver triflate, 2 g of graphite and 30 ml of diethyl ether under stirring for about 10 minutes. After evaporation of diethyl ether the column was prepared as fast as possible and placed protected from light into the system.

The introduction of a NaOH or P_2O_5/ascarite drying column (see Figure 4.4C-D) before [^{11}C]CH_3OTf production was tested to reduce traces of humidity in the tubing which can lead to greater amounts of [^{11}C]CH_3OH in the final product.

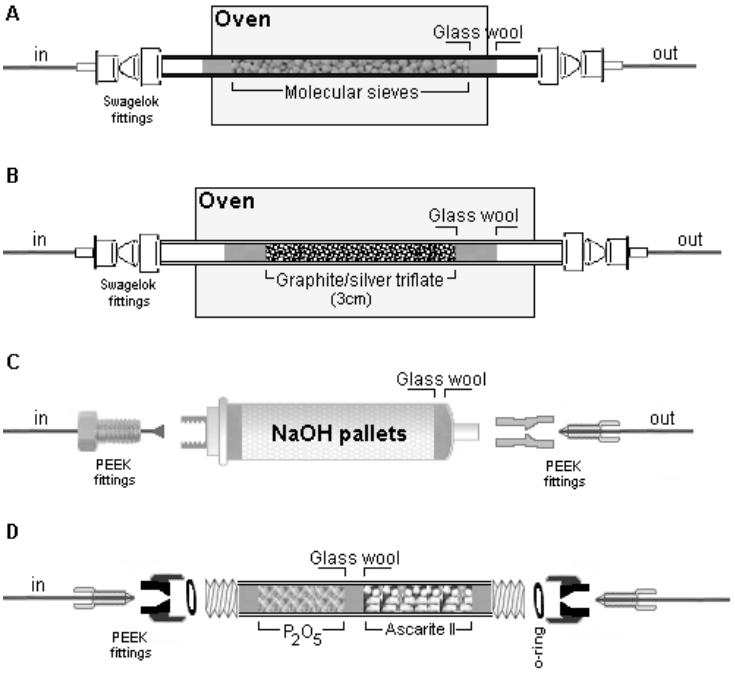

Figure 4.4. Columns used on the synthesis of [^{11}C]CH_3OTf.

4.2.3 Production of [^{11}C]PiB in a captive solvent loop

After being synthesized, the [^{11}C]CH_3OTf coming from the earlier automated methylation system was delivered by a nitrogen gas stream to a stainless steel reaction loop (1/16-inch outer diameter tubing, 2 ml of internal volume) maintained at room temperature and previously coated with the chemical precursor solution. The 6-OH-BTA-0 precursor was prepared in several solvents (MEK, DMF, DMSO, CH_3CN and acetone) and under different conditions (0.5 mg/80 µl, 1 mg/80 µl, 1 mg/100 µl and 1 mg/160 µl) to determine which yielded better results. After dissolving the precursor by stirring in a vortex the solution was promptly and slowly injected (5-10 s) into the clean dry AutoLoop^{TM} injector valve using an 100 µl Hamilton^{TM} syringe (Hamilton Company, Bonaduz, Switzerland).

Radioactivity trapped on the loop was detected by a proximal radiometric detector (see Figure 4.3) and after complete capture of the activity the loop was sealed and the

nitrogen flow stopped which allows the reaction to occur. In this work it was tested 1, 2, 3 and 4 minutes reaction time at room temperature.

The products of the reaction were then transferred, by passing a mobile phase of CH_3CN/H_2O (40/60) with 0.1 N NH_4HCO_2 through the loop with a flow rate of 9 ml/min, to a semi-preparative HPLC system to carry out the purification of the desired fraction.

4.2.4 Purification and reformulation of the final product

The crude product resulting from the reaction of 6-OH-BTA-0 with [^{11}C]CH_3OTf was carried by the mobile phase (CH_3CN/H_2O (40/60) + 0.1 N NH_4HCO_2, flow rate of 9 ml/min) through a HPLC semi-preparative Phenomenex® Luna C18(2) 5µ column (250x10 mm) installed in series with an UV detector set at 254 nm and a reformulation system (ReFORM-Plus™) with a radiometric detector for separation of the different chemical and radiochemical species.

After its retention time (r_t) has been identified previously by the HPLC injection of a cold standard, the desired [^{11}C]PiB peak was collected for reformulation into a physiological and sterile solution suitable for i.v. administration.

The reformulation process was established in a disposable 5-way stopcock manifold system installed at ReFORM-Plus™ (see Figure 4.3) and the flow of the solutions involved impelled by remotely controlled pressurization and/or vacuum of the desired compartments. After its separation and collection, the fraction containing [^{11}C]PiB was firstly diluted with 10-15 ml of WFI where it bubbled for a few seconds to ensure efficient mixing and then it was trapped in a SPE cartridge monitored by a radiometric detector. Three types of silica-based bonded phase SPE cartridges (C18 *Plus Light*, C18 *Plus Short* and *tC18 Plus Long* Sep-Pak from Waters®), previously hydrated and activated with ethanol, were tested for their ability to retain [^{11}C]PiB using the minimum amount of ethanol.

The SPE cartridge was then washed in 10-15 ml of WFI to remove the organic solvents from the mobile phase leaving only [^{11}C]PiB trapped due to its hydrophobicity which makes it hardly soluble in water. The loaded cartridge was successively eluted with 0.4-1.0 ml (according to the type of cartridge tested) of ethanol and 9 ml of NaCl 0.9% and sterilized by 0.22 µm filtration before reaching the sterile final vial. The amount of radioactivity of the final radiotracer was measured in a dose calibrator and a sample was subject to quality control.

In the end of each production cycle, a cleaning procedure was run to remove all residual radioactivity and chemicals in the modules. This cleaning procedure consists of passing ethanol, acetone and ether to wash the methyl iodide production system and water followed by ether and acetone in the reactor loop. A final drying step with nitrogen was performed in both modules and, after a new preconditioning of the molecular sieve column, the system was prepared for next synthesis.

4.2.5 Quality control

After measurement in a dose calibrator to calculate the radioactive yield, the final formulation of [^{11}C]PiB was subjected to a visual inspection. The solution examined should be clear and colourless with no visual evidence of cloudiness or particulate matter. Then, and according with the radiopharmaceutical preparations monograph of Ph. Eur., the pH of the solution was measured with a potentiometer to see if it has the value between 4.5 and 8.5 suitable for i.v. administration.

Chemical and radiochemical purity and identity were analyzed through a HPLC equipped with an UV and radiometric detector and a Zorbax Eclipse XDB-C18 column, 5 µm, 4.6x150 mm (Agilent Technologies©) using CH_3CN/H_2O (40/60) + 0.1 N NH_4HCO_2 as mobile phase with a flow rate of 4 ml/min. After verifying the stability of the analytical HPLC system the radiochemical identity of [^{11}C]PiB is confirmed if its r_t corresponds, with a small deviation resulting from the distance between the UV and radiometric detectors, to that of cold PiB standard solution previously injected.

To ensure the radiochemical purity, the area of the radioactive peak corresponding to [^{11}C]PiB shall represent more than 95% of the sum of all radioactive peaks areas existing in the chromatogram since potential radiochemical impurities, such as [^{11}C]CH_3OH, [^{11}C]CH_3I and [^{11}C]CH_3OTf, were removed during the semi-preparative HPLC purification.

Although radiochemical purity for radiotracers typically must be >95% there are currently no chemical purity requirements for their release in clinical research. Since potential non radioactive impurities in the final solution, such as the precursor 6-OH-BTA-0 and traces of $LiAlH_4$ not carried over during the distillation procedure or HI, were also eliminated by semi-preparative HPLC and C18 Sep-Pak the chemical purity should remain as high as the radiochemical. Therefore SA must be the main property to be evaluated.

Specific activity is the fraction of the radiotracer in relation to the total number of both radioactive and stable molecules of that same species (GBq/µmol) and is particularly relevant in PET radiotracers specifically directed to micromolar quantities of molecular targets. To quantify this property the area under [^{11}C]PiB UV mass peak was fitted to a standard calibration curve previously generated through several concentrations of cold PiB injected in the same HPLC system and related with the sample radioactivity.

Levels of organic volatile impurities were analyzed through the injection of 2 µl of the final solution into a gas chromatographer equipped with a FID and previously calibrated for the residual solvents in analysis. Since [^{11}C]PiB injection vehicle is 5% ethanol and 95% saline it is expected a prominent peak of ethanol in the chromatogram. By being part of the mobile phase the main residual solvent to be controlled is acetonitrile and its concentration in the final solution shall be, according to Ph. Eur., less than 4.1 mg/V where V is the maximum injected volume in ml.

Radionuclidic identity of the involved radioisotope was confirmed by measuring its $t_{1/2}$ across several assays in a dose calibrator. The final result was compared with the characteristic $t_{1/2}$ of ^{11}C (20.4 minutes) with a margin of ±5%.

The integrity of the 0.22 µm sterile filter was determined after use in the production of [^{11}C]PiB by the bubble point test (BPT). The sterile filter attached with the inlet needle to the final vial is also connected to a nitrogen supply regulator. After removing the final vial with the radiotracer the needle attached to the sterile filter is submerged in water and the nitrogen pressure gradually increased. It was considered that the filter guaranteed the sterility of the [^{11}C]PiB solution if the pressure was raised between the maximum value achieved during the reformulation process (typically 2 bar) and the limit supported and specified by the filter without seeing a stream of bubbles.

Finally, after i.v. administration of [^{11}C]PiB, the bacterial endotoxins content in the radiotracer was analysed using the *limulus* amebocyte lysate (LAL) test. This involves incubation (37º C) of the *limulus* lysate reagent (Charles River Laboratories EndoSafe®) with a sample of our solution for 60 minutes to determine if there was a potential contamination above 17.5 endotoxins units per ml.

The synthesized [^{11}C]PiB solutions were stored at room temperature in the original sterile vial sealed with a butyl rubber stopper and aluminium capsule for possible subsequent tests.

5.Results and discussion

The developed process aimed to obtain, in good yields, a final sterile and saline [^{11}C]PiB solution with a SA suitable to be used in human studies. Although the productions of [^{11}C]CH_3I by the "gas phase method" present higher specific activities they have the disadvantage of providing lower radiochemical yields. So, considering the characteristics of the "wet method" automated methylation system used, the main goal was to improve SA by reducing the global time of the synthesis and increasing the radiochemical yield which, consequently, may raise the final specific activity.

All experiments were performed at least 3 times (*n*=3), to achieve a minimally acceptable level of confidence, and mostly carried out through long irradiation periods (integrated current of approximately 12 µAh during 30 minutes) to create the same conditions for a production destined to clinical use. Shorter productions could facilitate the collection of data but, when extrapolated to the bigger ones required to reach the necessary activity for human studies, might introduce a possible error associated with the particular conditions submitted in the cyclotron target. Actually is widely accepted that, for example, by varying the beam current and the irradiation time, different sources of carrier carbon have to be considered[105, 106].

5.1 Chromatographic system

Due to its short $t_{1/2}$, the synthesis of ^{11}C labelled radiotracers must be performed as quickly as possible. Commonly this process is particularly optimized during the chemical reaction steps but efforts should be made also to refine the chromatographic system since a long separation time, either during the purification or the checking of the quality parameters prior to administration, will obviously limit the total radioactivity of the radiotracer available.

From the selected mobile phase CH_3CN/H_2O (40/60) with 0.1 N NH_4HCO_2, and knowing that generally the introduction of a methyl group in a molecule increases its lipophilicity, we used reversed phase C18 HPLC columns both in the analytical (Zorbax Eclipse XDB-C18, 5 µm, 4.6x150 mm) and semi-preparative (Luna C18(2), 5 µm, 10x250 mm) systems. The separation mechanism through reversed phase chromatography depends on the hydrophobic binding interaction between the solute molecule in the mobile phase and the stationary phase. In our case this last one is

composed by an octadecyl carbon chain (C18) bonded in silica. This highly efficient stationary phase for hydrophobic compounds which, for having lower polarity than that used in normal phase chromatography allows the use of less toxic mobile phases composed by common organic solvents of high polarity, is particularly suitable for an appropriate separation of molecules intended for i.v. administration.

Because in radiochemical synthesis the precursor is always used in large excess, a considerable amount of this product is expected at the final crude mixture. To prevent a predictable and severe tailing effect of this major peak in the chromatogram, able to mask and contaminate the peak of the compound of interest that is intended to separate and collect, we need to ensure a sufficient difference between each retention time (r_t) so that there is no overlap of the two species since this would irreversibly affect the purity of the final product.

After the individual identification by analytical HPLC of the cold reference standards of 6-OH-BTA-0, CH_3I and PiB in different flow rates it was concluded that the one that had shorter r_t, in order to prolong the chromatographic run as least as possible, and enough resolution to be capable to separate the various compounds making them easily distinguished and identified, was 4 ml/min (6-OH-BTA-0 r_t=0.94±0.04 min, CH_3I r_t=1.43±0.06 min, PiB r_t=1.82±0.09 min). To confirm the selection of these parameters we also injected a mixture of different concentrations of each reference standard to better understand the separation achieved between the three solute molecules (see Figure 5.1).

The same procedure was repeated for the semi-preparative system where we used the highest flow rate possible, taking into account the maximum pressure supported by the installed HPLC column (22 bar). With a flow rate of 9 ml/min we obtained r_t of 3.71±0.11 min, 5.83±0.18 min and 6.88±0.44 min for 6-OH-BTA-0, CH_3I and PiB, respectively (see Figure 5.2).

An adequate HPLC resolution, generally defined as the distance between the centres of two eluted peaks divided by the average width of the respective peaks, is particularly essential at semi-preparative systems since it is important to ensure that by collecting 100% of the interesting peak we will get it theoretically with 100% of purity. This has major interest in the need to ensure that the collected peak corresponding to [^{11}C]PiB is free of impurities which would reduce the final chemical and radiochemical purity of the final solution. Of these impurities, we must take into account particularly the ones

related to the precursor 6-OH-BTA-0 that, due to their biological activity, can compete *in viv*o for the same target.

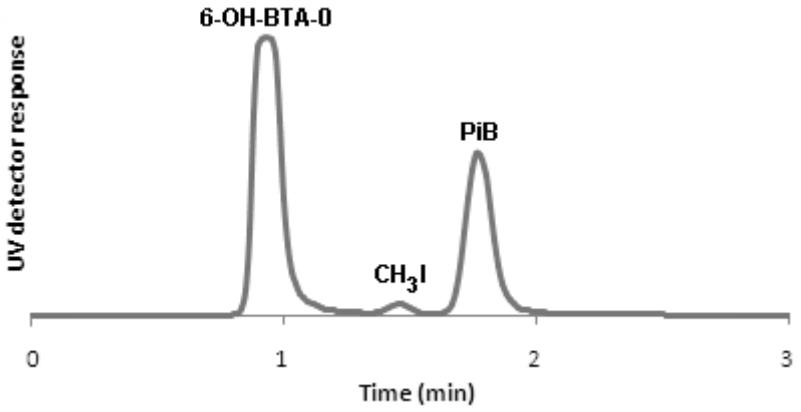

Figure 5.1. Analytical HPLC of cold standards mixture.

The calculated resolution achieved between PiB and its precursor with the chosen chromatographic system was approximately 4, which ensures total purity of the collected specie over the other. The distance to the CH_3I peak is not as critical since this one is efficiently eliminated from the final radiotracer solution by subsequent SPE.

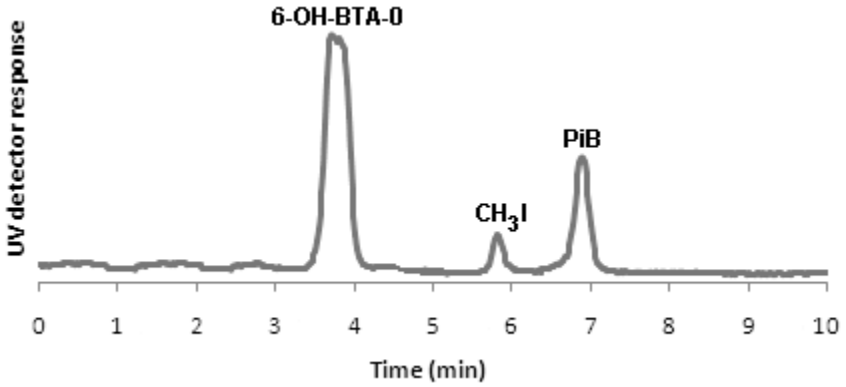

Figure 5.2. Semi-preparative HPLC of cold standards mixture.

Summarizing, the chromatographic conditions used during all purification and quality control process were, an isocratic CH_3CN/H_2O (40/60) + 0.1 N NH_4HCO_2 mobile phase, a flow rate of 9 ml/min with a Luna C18(2) HPLC column (5 µm, 10x250 mm), for the

semi-preparative, and a flow rate of 4 ml/min with a Zorbax Eclipse XDB-C18 HPLC column (5 µm, 4.6x150 mm), for the analytical system.

By injecting in the analytical HPLC system 4 replicates of 3 different known concentrations of the cold PiB standard we constructed a reference curve in order to subsequently infer, through the UV peak area corresponding to PiB fraction, the concentration of the final radiotracer solution (see Figure 5.3). From this value and from the known total activity and final volume we are able to calculate SA of [^{11}C]PiB after synthesis and before injection time.

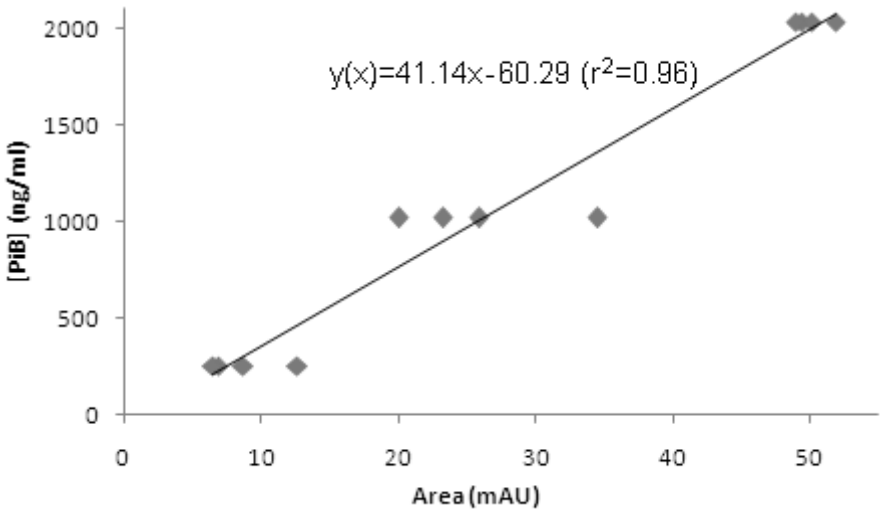

Figure 5.3. Reference curve for the calculation of PiB concentration.

5.2 Synthesis of [^{11}C]CH_3I and conversion into [^{11}C]CH_3OTf

Since 1976, when it was first prepared to synthesize [^{11}C]methionine, [^{11}C]CH_3I is the most common secondary radioactive precursor used for ^{11}C radiolabelling[107]. The used commercial automated methylation system allow its preparation by the very reliable “wet method” where [^{11}C]CO_2 is firstly reduced to [^{11}C]CH_3OH, by action of $LiAlH_4$, and then reacts with HI in order to generate [^{11}C]CH_3I (see Figure 5.4).

Although being a very efficient method that leads to appreciable absolute quantities of [^{11}C]CH_3I, this technique however suffers from the drawback of relying on the relationship between the produced [^{11}C]CO_2 and the atmospheric CO_2 existing in the reaction environment, which normally results in low specific activities.

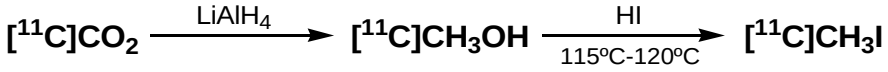

Figure 5.4. Synthesis of $[^{11}C]CH_3I$ by the "wet method".

Knowing that the contamination of the cyclotron target and gas lines with $[^{12}C]CO_2$ is practically unavoidable, leading to a theoretical contamination of 100-1000 atoms of stable carbon for each ^{11}C atom produced[33], is important to reduce all other contamination factors that can be more easily controllable. Procedures to reduce the amount of "cold" CO_2 that enters in the system, like the introduction of an ascarite trap between the N_2 supply and the MeI-Plus™ module or a routine search for leaks, can bring significant results. However several authors have been pointing $LiAlH_4$/THF solution as the main source of this contaminant[106, 108, 109].

In fact the use of $LiAlH_4$/THF can be the critical point to obtain higher specific activities since the formation of non-radioactive species may occur prior to its introduction in the automated system by reduction with environmental CO_2 during handling or improper storage. Once *in situ* preparation of $LiAlH_4$ dissolved in dry THF requires strict conditions of inert atmosphere, the adopted option during the development of this project was to use 0.1 M commercially available sealed solutions (with a background of less than 5 ppm of $[^{12}C]CO_2$) released in lower volumes so that can be discarded after each perforation of the vial rubber stopper when used in the automatic $[^{11}C]CH_3I$ production module.

The central oxygen of THF eventually remaining after evaporation can also react with $LiAlH_4$ hydride ions originating carrier carbon under the form of methanol. Ways to counteract this chemical effect include doing an efficient THF evaporation (3 to 4 minutes at 115º-120º C proved, through visual check, to be sufficient for the absence of droplets residues in the reactor while lower temperatures, for example 105º C, revealed some presence of aqueous substances), maximizing the concentration of the $LiAlH_4$/THF solution (in the presented study we used a 0.1 M solution but there is also commercially available an 1.0 M formulation, so the results using this higher concentration could be evaluated in the future) or reducing the release in the reactor vessel of this reagents to the minimum amount possible without affecting $[^{11}C]CO_2$ trapping or $[^{11}C]CH_3I$ production after treatment with an excess (350-450 µl) of HI.

To optimize this last parameter a set of experiments were carried out in order to reach the minimum volume of $LiAlH_4$ in dry THF (0.1 M) that must be used to an effective trapping of $[^{11}C]CO_2$ and further production of $[^{11}C]CH_3I$ (see Table 5.1).

Table 5.1. $LiAlH_4$ volume influence in $[^{11}C]CO_2$ trap and $[^{11}C]CH_3I$ production.

$LiAlH_4$/THF (0.1 M) volume	**Yield of $[^{11}C]CO_2$ trapping***	**Yield of $[^{11}C]CH_3I$ production***
250 µl (*n*=3)	93.8±4.1%	77.9±5.1%
200 µl (*n*=5)	90.3±2.3%	72.0±9.3%
150 µl (*n*=3)	88.1±2.3%	73.2±3.2%
100 µl (*n*=4)	92.1±4.5%	77.5±3.5%
75 µl (*n*=3)	89.9±5,8%	77.4±4.1%

*Decay corrected (DC) values

It was observed that the volume of $LiAlH_4$ employed does not significantly affect the quantity of $[^{11}C]CO_2$, coming from the molecular sieve column, that is trapped in the reactor vessel. After reaction with HI the yields of production of $[^{11}C]CH_3I$ also remained practically constant (note that these values take into account possible radiochemical impurities, such as unreacted $[^{11}C]CH_3OH$, which may be present in the reactor crude mixture and cannot be separated) between a $LiAlH_4$ volume of 75 to 250 µl. The release of radioactivity from the molecular sieve column and the follow up of its dynamics in the reactor vessel were monitored by radiometric detectors (see Figure 5.5).

Since it is known that the decrease of the quantity of $LiAlH_4$/THF is a critical point that inversely affects final SA of a radiotracer[109] it was selected a volume between 75 to 125 µl for the synthesis of $[^{11}C]CH_3I$. This range of values was chosen to take into account a possible error inherent to the automatic dispenser of the MeI-Plus™ system, because when selecting strictly 75 µl it would be a risk that the released volume was lower than the expected.

After synthesis, the resulting $[^{11}C]CH_3I$ is dried and separated from some side products by distillation under continuous nitrogen flow (approx. 3 minutes at 115º-120º C). Distillation is a separation method based on the vapour-liquid equilibrium

phenomenon that allows that two or more substances, with different volatilities, forming a liquid mixture can be isolated. However [^{11}C]CH_3OH (boiling point of 65º C), the more relevant radiochemical impurity, remains blended in [^{11}C]CH_3I (boiling point of 43º C) since the distillation temperature makes both compounds gaseous. A decrease in temperature to a value between the two boiling points is not a viable alternative because it turns the distillation process of [^{11}C]CH_3I too slow, which is inconsistent with the indispensable quickness when working with ^{11}C, and, furthermore, it is also reported that a distillation temperature lower than 110º does not lead to the formation of any product[99]. So, as will be discussed, a subsequent separation by semi-preparative HPLC is a more efficient process to remove [^{11}C]CH_3OH from the final solution.

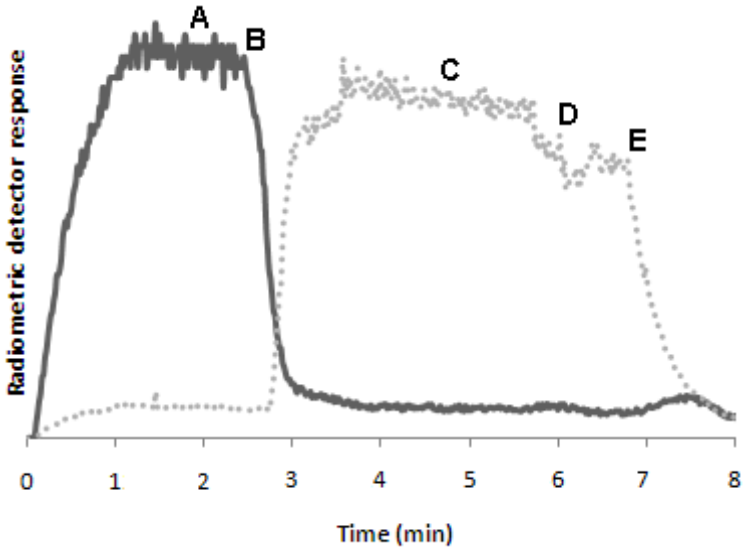

Figure 5.5. [^{11}C]CH_3I production profile. (A) maximum [^{11}C]CO_2 trapping after cyclotron production. (B) beginning of [^{11}C]CO_2 release by heating; (C) maximum [^{11}C]CO_2 trapping by reduction of $LiAlH_4$; (D) THF evaporation followed by HI reaction; (E) maximum level of [^{11}C]CH_3I produced and beginning of distillation. Molecular sieve detector (solid line) and reactor detector (dotted line) profiles are shown.

Once 6-OH-BTA-0 does not react at room temperature with [^{11}C]CH_3I (all experiments carried out at these conditions did not lead to the formation of [^{11}C]PiB) the reactivity of the electrophilic carbon of this radioactive precursor was improved by preparing the methylation agent [^{11}C]CH_3OTf. For this, the distilled [^{11}C]CH_3I was passed in a

nitrogen flow through a conversion column, filled with graphite and silver triflate and preheated at 180º C, to suffer a quantitative reaction (virtually 100% yield).

Between the distillation and the conversion column two types of drying columns were tested since the possible presence of traces of gaseous HI can react with oxygen originating H_2O molecules that, in contact with $[^{11}C]CH_3OTf$, can lead again to the formation of the radiochemical impurity $[^{11}C]CH_3OH$. A drying column formed by P_2O_5 (that removes traces of H_2O) and ascarite (a trap for the excess of HI) revealed to be more efficient than the NaOH column commonly reported in literature. The removal of acid and water is necessary for a good methylation yield and the distillation via P_2O_5/ascarite trap shown to lead to lower amounts of $[^{11}C]CH_3OH$. This was observed at semi-preparative HPLC chromatogram where $[^{11}C]CH_3OH$ have a r_t of 1.56±0.35 minutes (see Figure 5.6). In all experiments performed the formation of this by-product was directly associated with residual humidity present on the lines and columns. For that reason before the first daily synthesis all lines, including the one passing through the column in triflate oven, were dried with a nitrogen flow.

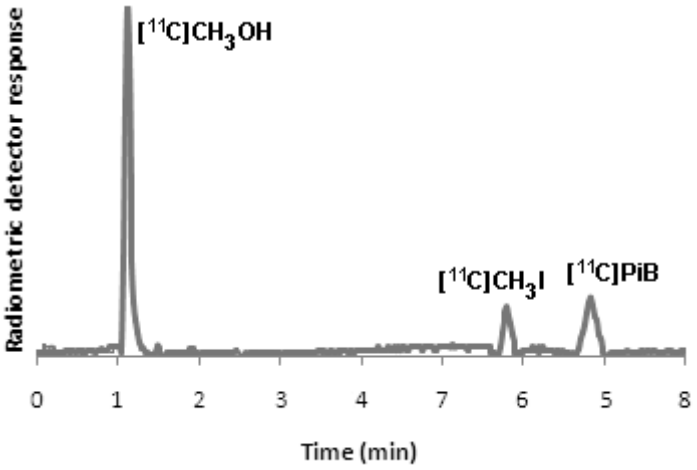

Figure 5.6. Semi-preparative HPLC of $[^{11}C]$PiB and main radiochemical impurities.

The preparation of the conversion column is also quite important since a poor homogenization of graphite and silver triflate mixture may cause an incomplete conversion of $[^{11}C]CH_3I$ which, although not reacting with 6-OH-BTA-0 precursor to form $[^{11}C]$PiB, will be an additional radiochemical impurity in the final crude mixture

(see Figure 5.6). An excessive compression of that mixture also proved to be problematic as it could lead to an inexistent or excessively slow conversion rate of $[^{11}C]CH_3OTf$ due to the inability of the nitrogen flow carrying $[^{11}C]CH_3I$ to efficiently cross the column.

This optimization of the $[^{11}C]CH_3I$ synthesis process and subsequent conversion to $[^{11}C]CH_3OTf$ is an essential step to move forward toward 6-OH-BTA-0 radiolabelling.

5.3 The reaction by the captive solvent method

Iwata *et al.*[108] concluded that, after ensuring the care in $LiAlH_4$/THF handling and reducing its volume to the minimum possible, further optimization of the SA values are difficult to obtain. So, the increasing of starting ^{11}C activity, the optimization of reaction conditions to get higher yields and the shortening of synthesis time will be the most appropriate solutions to get better results.

Using the captive solvent method the trapping and reaction of $[^{11}C]CH_3OTf$ with the chemical precursor occurs directly in the injection loop of a HPLC allowing a rapid release of the crude mixture in the purification system. The major advantage of this method lives in the loop geometry that allows to reduce drastically the solvent volume (compared to bubbling reaction in vessels), increasing the concentration of the precursor solution, leading to fast rates of reaction at room temperature and neutral conditions. Since no vials, transfer lines, cooling, heating, or sealing valves are required, no transfer losses occur, yields are high, and the contamination is minimal, this method is ideal for the rapid preparation of $[^{11}C]$radiotracers[89].

After $[^{11}C]CH_3OTf$ conversion the activity leaves the column filled with graphite and silver triflate and reaches the reaction loop pre-filled with a solution of the chemical precursor. This phase is monitored by a radiometric detector installed at the centre of the loop and another one in a trap near the exhaust to control the activity lost (see Figure 5.7).

The choice of the solvent used to dissolve the chemical precursor may affect the final yield as it has the function of retaining the $[^{11}C]$methylation agent but can also bring potential impurities associated to it (e.g., cyclohexanone needs to be previously dried with $MgSO_4$[101]). So we tested some of the most common solvents used in $[^{11}C]$radiolabelling (MEK, DMF, DMSO, CH_3CN and acetone) to evaluate their trapping capacity and the ability to enhance the reaction (for 1 minute) with the precursor. After

stirring 0.5 mg of 6-OH-BTA-0 with 80 µl of solvent this was immediately injected into the loop to avoid evaporation as a dry precursor is unable to react with [^{11}C]CH_3OTf.

DMF is a commonly used solvent for methylation reactions with [^{11}C]CH_3I mainly due to its high boiling point (153º C). Nevertheless, our results showed a great escape of the activity from the loop resulting in an absent production of [^{11}C]PiB. This can be explained by direct reaction of [^{11}C]CH_3OTf with DMF, and is by-product dimethylamine, forming [^{11}C]trimethylamine which has a boiling point of 3º C. So, the use of DMF as solvent for our methylation with [^{11}C]CH_3OTf was promptly discarded.

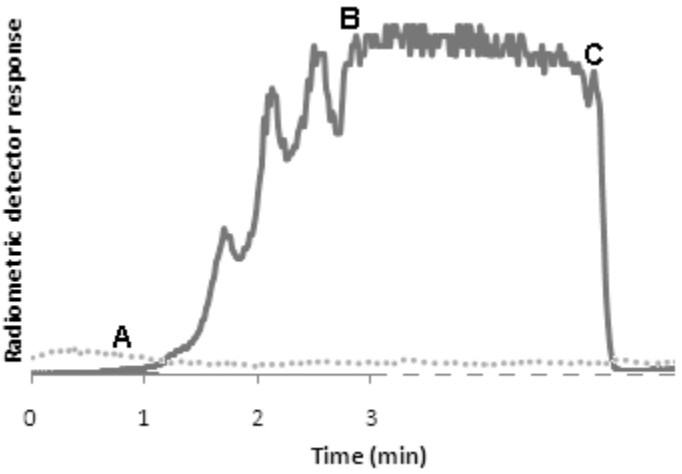

Figure 5.7. Optimum profile for [^{11}C]CH_3OTf trapping in the loop. (A) start trapping; (B) maximum trapping and beginning of the reaction with 6-OH-BTA-0; (C) end of the desired time of reaction and transfer to semi-preparative HPLC for purification of the crude mixture. Loop detector (solid line) and exhaust trap detector (dotted line) profiles are shown.

When a [^{11}C]methylation is done with [^{11}C]CH_3I, in presence of a strong base that catalyses the chemical precursor deprotonation, DMSO is one of the widely used solvents also due to its high boiling point (189º C). However, since the sulphur atom in DMSO is by itself a nucleophilic centre, the solvent may compete with the dissolved precursor when using the more reactive methylation agent [^{11}C]CH_3OTf especially if a base is not used[110]. This reaction between DMSO and [^{11}C]CH_3OTf leading to [^{11}C]methylated DMSO was potentially observed in some of the experiments that used these conditions for 6-OH-BTA-0 radiolabelling. Here, during the semi-preparative

HPLC, there is a radioactive species around the area where the DMSO peak is expected, as previously identified by the UV detector (see Figure 5.8). This causes, despite the good trapping in the loop (74.6±16.4%, *n*=3), a low radiolabelling yield of 4.3±2.9% (DC) due to the [^{11}C]methylation competition between precursor and solvent. This way, the use of DMSO was also set aside.

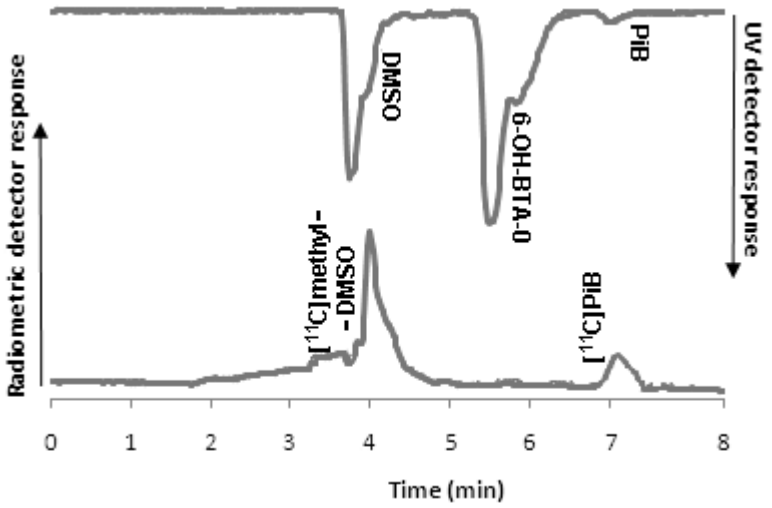

Figure 5.8. Semi-preparative HPLC of [^{11}C]PiB methylation using DMSO.

For methylations with [^{11}C]CH_3OTf the most commonly used solvent is acetone(111). However for loop reactions, where smaller amounts of solvent are employed, acetone is considered too volatile (boiling point of 56º C) to be used. This assumption was verified experimentally in our work where the loop trapping of the [^{11}C]CH_3OTf was about 25.5±19.9% (*n*=4) but then there was a good [^{11}C]PiB reaction yield of 18.3±7.4% (DC).

In order to overcome this volatility problem maintaining the promising reaction yield achieved, Gómez-Vallejo and Llop(101) tested, with good results, a mixture of acetone/CH_3CN (1/1) as solvent. When we also tested this solvent (firstly diluting 6-OH-BTA-0 with acetone and then adding the remainder of CH_3CN, otherwise it was noted the formation of a precipitate between precursor and CH_3CN) we obtained a [^{11}C]CH_3OTf trapping efficiency of 69.3±8.6% (*n*=5) with a reaction yield of 22.6±4.3% (DC).

There are however a series of other less volatile ketones which may be used to dilute the precursor. Several [^{11}C]methylations of various radiotracers have been made using MEK (boiling point of 80º C) as solvent and for this reason there was great interest to test it in the present work. The results obtained by diluting precursor in MEK showed a yield of [^{11}C]CH_3OTf trapping in the loop of 35.2±5.0% (*n*=3) and a following reaction yield of 15.5±7.9% (DC), which is in agreement with the [^{11}C]PiB reaction yields reported in literature (11 to 18%) when using this solvent[97, 99].

In summary, on our tests the use of acetone/CH_3CN (1/1) showed to improve the trapping efficiency of [^{11}C]CH_3OTf in the loop and the [^{11}C]PiB reaction yield. For this reason all experiments described hereafter were made using this solvent.

Another factor that can vary the yield of 6-OH-BTA-0 [^{11}C]methylation is the quantity of precursor and solvent used. Considering that the precursor is always used in large excess on radiolabelling reactions we tested the amounts of 0.5 to 1 mg and the influence of solvent volumes between 80, 100 and 160 µl (see Table 5.2). The solvent volume was not increased too much in order to not pervert one of the main assumptions and advantages of the loop captive solvent method which is to use the lowest volume possible. The reaction time in this experimental segment was set constant to 1 minute.

Table 5.2. Precursor dilution influence in [^{11}C]PiB reaction yield and specific activity.

Precursor dilution	Yield of [^{11}C]PiB production*	Specific activity (GBq/µmol)**
0.5 mg/80 µl (*n*=4)	22.6±4.3%	16.7±5.9
1 mg/80 µl (*n*=3)	21.1±4.2%	20.4±6.6
1 mg/100 µl (*n*=3)	19.0±2.1%	17.2±1.5
1 mg/160 µl (*n*=3)	15.1±3.1%	17.3±0.7

*DC and **End of synthesis (EOS) values

Analyzing this results we can infer that lower volumes of acetone/CH_3CN (1/1) leads to better yields of [^{11}C]PiB production. This may be due to the fact that by reducing solvent volume we are also reducing potential impurities contained in them, particularly

traces of H_2O, which will limit the production of by-products like [^{11}C]methanol. With the dilution 1 mg/80 µl it was achieved the best results for SA.

Finally, and using the best conditions of 1 mg of 6-OH-BTA-0 diluted in 80 µl of acetone/CH_3CN (1/1), we tested the influence of reaction time in final [^{11}C]PiB yield and in the obtained SA (see Table 5.3).

Table 5.3. Reaction time influence in [^{11}C]PiB production yield and specific activity.

Reaction time (minutes)	Yield of [^{11}C]PiB production*	Specific activity (GBq/µmol)**
1 (*n*=3)	21.1±4.2%	20.4±6.6
2 (*n*=4)	23.5±6.8%	27.2±4.5
3 (*n*=4)	15.7±4.1%	20.3±0.8
4 (*n*=3)	18.4±3.9%	16.2±1.5

*DC and ** EOS values

Through the optimization of the solvent, precursor dilution and reaction time it was possible to identify that the reaction conditions which lead to better results in the commercial system used in this work were: 1 mg of 6-OH-BTA-0, diluted firstly in 40 µl of acetone and then completed with more 40 µl of CH_3CN, allowed to react with [^{11}C]CH_3OTf at room temperature during 2 minutes (see Table 5.4).

Table 5.4. Optimal [^{11}C]PiB reaction conditions and comparison with several authors.

Reaction temperature	Reaction time (minutes)	Precursor quantity (mg)	Solvent (volume)	Yield of [^{11}C]PiB production	Specific activity (GBq/µmol)	Reference
Room temperature	2	1.0	Acetone/CH_3CN (80 µl)	23.5±6.8%	27.2±4.5	---
60º C	2	0.5	Acetone (400 µl)	14.5%	0.037	Mikhno *et al.*[98]
80º C	1	1.0	MEK (2 ml)	18%	9.3	Cheung and Ho[99]
Room temperature	1	1.0	Cyclohexanone (80 µl)	13-15%	20-60	Verdurand *et al.*[104]
20º C	1	0.4	MEK (250 µl)	11-16%	30-60	Wilson *et al.*[97]

However, to obtain a high chemical and radiochemical purity [^{11}C]PiB solution with the suitable characteristics for human i.v. administration, it is also mandatory to carry out an optimization of the commercial reformulation system (ReFORM-Plus^{TM}) installed after semi-preparative HPLC purification process, as will be discussed below.

5.4 Final purified saline solution of [^{11}C]PiB

Through the semi-preparative HPLC it was possible to carry out a purification of the compound of interest, in this case [^{11}C]PiB (r_t of 6.88±0.44 min), by collecting it separately from other species in the mixture (see Figure 5.9) and trapping it in a C18 silica-based bonded phase cartridge, monitored with a radiometric detector, installed in a disposable 5-way stopcock manifold at ReFORM-Plus^{TM} (see Figure 4.3).

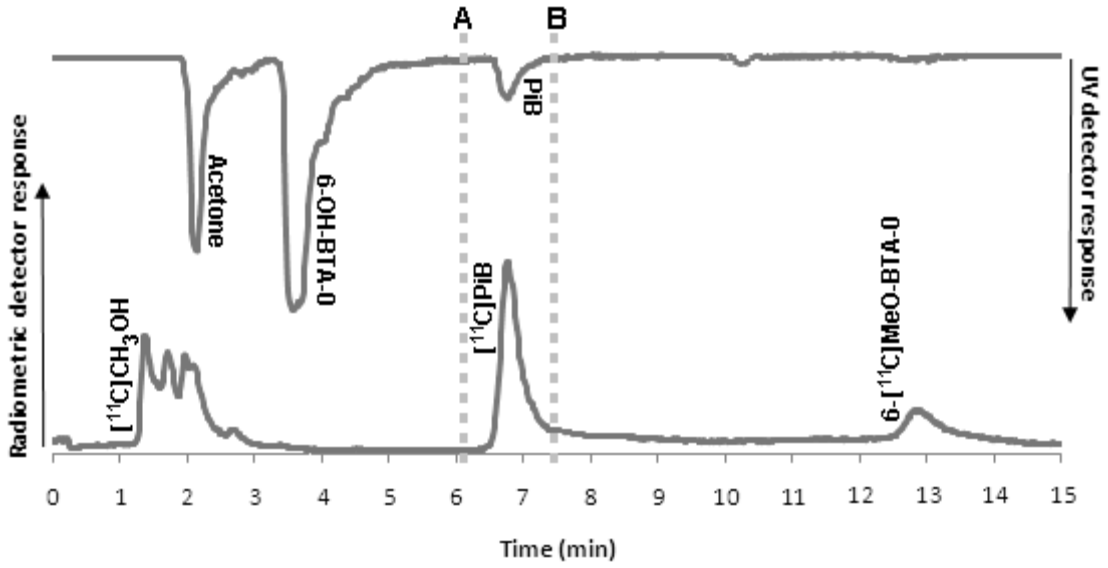

Figure 5.9. Semi-preparative HPLC for purification of [^{11}C]PiB. (A) start of peak collection; (B) stop peak collection and beginning of reformulation.

Not surprisingly high quantities of [^{11}C]CH_3OH were produced in parallel with [^{11}C]PiB since [^{11}C]CH_3OTf is extremely sensitive to water leading preferentially to the radiosynthesis of this radiochemical impurity. The amount of this impurity can be controlled with the care of keeping all system lines dry.

Sep-Pak C18 cartridges were designed to adsorb hydrophobe analytes from aqueous solutions ensuring reproducible separations. The octanol-buffer partition coefficient (log *P*) is a measure of the lipophilicity of a compound (log *P* >0 characterize hydrophobic substances soluble in a lipid phase, while log *P* <0 typifies polar compounds soluble in a water phase) and since [^{11}C]PiB log *P* is 2.48±0.063[112] it has the physicochemical characteristics to suffer retention in that SPE system.

However, by passing the collected fraction directly from the HPLC to the C18 SPE cartridge with a flow rate of 9 ml/min, as intended in the original commercial system, we observed that the retention in the column was very poor which caused heavy losses in the final amount of the obtained radiotracer. So a change has been implemented in the system to make the collected fraction to be diluted first in a vial with 10-15 ml of WFI and only then slowly passed through the SPE cartridge (see Figure 5.10). By doing this procedure the losses of radiotracer were considered insignificant since practically all the monitored activity was retained in any of the columns tested. The difference between C18 *Plus Light* (130 mg, 55-105 µm), C18 *Plus Short* (360 mg, 55-105 µm) and *tC18 Plus Long* (900 mg, 37-55 µm) Sep-Pak is in the quantity of silica per cartridge and its particle size. These particularities will affect the absorptive capacity of each one and so the volume of eluent needed.

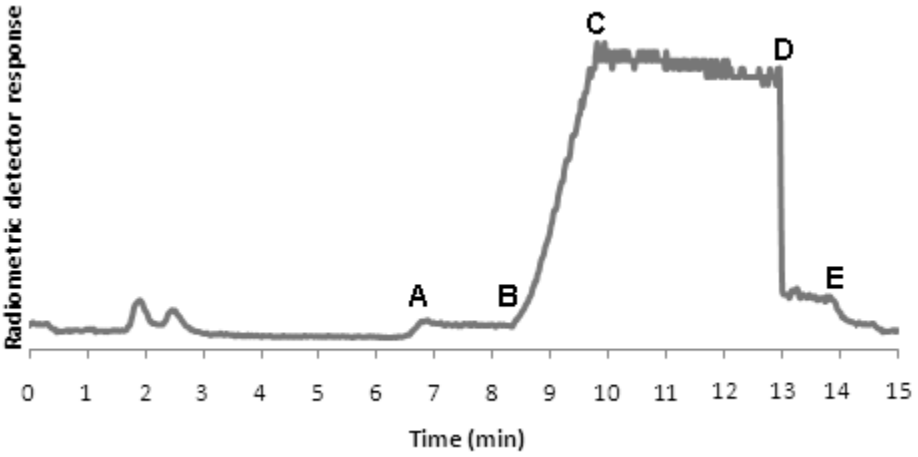

Figure 5.10. SPE C18 cartridge profile during [^{11}C]PiB purification. (A) collection of [^{11}C]PiB peak (see Figure 5.9) to the dilution vial; (B) start of trapping in C18 sep-pak cartridge; (C) maximum [^{11}C]PiB trapping and washing with WFI; (D) elution with a volume of ethanol and beginning of collection at final product vial; (E) final washing of the cartridge and dilution with NaCl 0.9%.

To better wash each column from CH_3CN and NH_4HCO_2, coming from the mobile phase where [^{11}C]PiB was diluted, they were eluted with 10-15 ml of WFI. Thus, in the C18 columns, we only expect to retain the radiotracer and minor trace amounts of CH_3CN (which will be quantified by GC to ensure that the achieved values are within the limits allowed for i.v. administration).

To recover the product trapped it is necessary to elute the C18 cartridge with a certain volume of ethanol collecting it on the final product vial. However, since ethanol will carry out [^{11}C]PiB to the final injectable solution thus becoming a part of it, it is necessary to optimize this process by selecting the cartridge which requires the lower volume of this solvent to be fully eluted with minimum losses of the radiotracer. This way, the tested cartridge that had the best result was C18 *Plus Light*. This SPE column proved to be completely eluted with a volume of 0.3-0.5 ml, while *tC18 Plus Long* and C18 *Plus Short* need an amount between 0.6 and 1.0 ml to achieve the same results.

After reaching the final product vial, ethanol containing [^{11}C]PiB is diluted by 9 ml of NaCl 0.9% (that also passes through C18 column to wash the trace amount of radioactivity still remaining there) to turn the solution in a physiologically injectable one.

Immediately before any solution enter into the final product vial, it is purified by a sterilizing disposable filter unit to remove microorganisms, particles, precipitates and other undissolved components larger than 0.22 µm. This procedure is indispensable for non-pyrogenic i.v. administration solutions prepared *in situ* and therefore two kinds of sterilizing filters (Millex®-GS for aqueous solutions and Millex®-GV for aqueous or mild organic solutions) were tested. By passing the same [^{11}C]PiB solution through the two filters it was observed that Millex®-GV is the most appropriate for purification and sterilization of the final product being suitable for hydrophobic compounds since it only retains 8.9±2.9% of the final solution activity while in Millex®-GS there are higher losses as it retains 20.8±18.1%. After filtration of the final solution it has to be done a BPT to verify filters integrity.

In a set of 12 radiolabelling and reformulation experiments, that were made after defining the optimal conditions (see Table 5.5), it was obtained an absolute [^{11}C]PiB reaction yield of 23.5±6.8% (after sterile filtration), referred to [^{11}C]CH_3I (DC), with a SA of 27.6±4.1 GBq/µmol. The observed formation of the non collected 6-[^{11}C]MeO-BTA-0 specie was about 5.9±1,6% and, at EOS, 3.2±1.2 GBq of pure [^{11}C]PiB were obtained with a total synthesis time between 25 to 30 minutes. Therefore, the values of SA reached in this project, as well as the yields of [^{11}C]PiB production, are higher or

amongst those described in literature that also uses “wet method” for producing the primary radioactive precursor [^{11}C]CH_3I (see Table 5.4).

The consideration of SA, as already described, is particularly important in the production of a radiotracer and its degree must be addressed depending on the nature of the molecular target in study. According to a recent paper from Manook *et al.*[113] a value between 11.1 and 14.8 GBq/μmol proved to be sufficient for routine applications in [^{11}C]PiB molecular imaging of AD patients. So, after quality assurance, the synthesised product has all the conditions to be used in human clinical assays.

5.5 Assurance of the final product quality

Intravenous administration of a radiotracer must comply with both radiation and pharmaceutical standards not only to ensure safety but also to establish its efficiency since the *in vivo* behaviour is dependent on high levels of radionuclidic, radiochemical and chemical purity. In addition, injectable solutions must also satisfy other standards of sterility, apyrogenicity, osmolarity and pH to ensure the safe administration in humans. These parameters are detected and quantified using analytical techniques according to the general radiopharmaceutical preparations monograph of Ph. Eur.

So far, not a single complete process of synthesis and reformulation of [^{11}C]PiB failed and in all cases a visual inspection of the final solution proved that it meets the organoleptic characteristics of being clear, colourless and free of particulate matter.

From the set of 12 synthesis and reformulation under the optimized conditions, all the obtained solutions complied with the parameters of quality assurance (see Table 5.5). After measurement of the EOS activity in a dose calibrator a small sample was taken to proceed to the pH test. The average pH of the solutions was 5.8±0.7 which is in agreement with the Ph. Eur. referenced range for radiopharmaceutical injection solutions (4.5-8.5).

Radionuclidic purity, defined as the percentage of the radioactivity of the required radionuclide to the total radioactivity of the solution[114], as well as its identity were assessed by $t_{1/2}$. The rate at which a radioactive isotope decays is measured in half-life, a particular physical property of each one that allows their identification. A deviation of more than 5% of the expected value (20.4 minutes for ^{11}C) may indicate the presence of other radioisotopes and the performance of several measurements over time of the activity of samples taken from each [^{11}C]PiB synthesized showed always a $t_{1/2}$ within

this range. This is important to ensure that will be prevented an unnecessary irradiation of the patient and to avoid a possible degradation of image quality.

Table 5.5. Results obtained with [^{11}C]PiB radiolabellings.

	Activity EOS (GBq)	Specific activity (GBq/μmol)	[CH_3CN] (mg/10ml)	pH	$t_{1/2}$ (min)	Chemical purity (%)	Radiochemical purity (%)
1	0.4	27.4	2.2	5.5	20.3	99.4	97.1
2	3.5	23.9	1.0	5.3	20.4	99.4	99.5
3	4.7	31.7	0.9	5.2	21.2	99.7	99.4
4	3.8	22.8	1.1	5.8	20.5	99.4	95.2
5	4.1	32.0	0.4	5.6	20.6	99.4	99.1
6	4.2	30.0	1.3	5.8	20.4	98.7	99.4
7	2.9	28.1	1.1	5.6	20.6	99.1	98.4
8	3.9	26.0	1.5	5.3	20.6	99.7	98.5
9	3.6	23.9	0.9	5.5	20.4	98.1	95.1
10	3.2	21.3	1.5	5.8	19.7	99.6	96.2
11	1.4	34.5	3.6	7.6	20.4	97.6	95.4
12	3.2	30.0	2.8	6.4	20.4	99.5	98.1
$\bar{x} \pm \sigma$	3.2±1.2	27.6±4.1	1.6±0.9	5.8±0.7	20.5±0.4	99.1±0.7	97.6±1.8

Levels of residual solvents in final solutions were quantified by GC/FID (see Figure 5.11). Since [^{11}C]PiB injection vehicle is 5% ethanol (95% NaCl 0.9%) and acetonitrile forms part of the mobile phase these are the two possible organic volatile impurities that may be present in an i.v. radiotracer dose within the limits described at Ph. Eur. (ethanol ≤50 mg/10 ml; CH_3CN ≤4.1 mg/10 ml).

All CH_3CN values obtained with the final solution were below the limit of 4.1 mg/10 ml which means that, assuming a maximum injection volume of 10 ml, 4.1mg were injected in a standard 70 kg human. This would result in a dose of about 60 μg/kg well below the LD_{50} (a standardized measure for expressing and comparing the toxicity of chemicals defined as any dose that kills 50% of the test animals) for CH_3CN administered i.v. in rats (1.68 mg/kg[115]). With regard to ethanol, the maximum amount used to elute C18 *Plus Light* cartridge was 0.5 ml or 0.4 g (assuming a density of 0.8 g/ml at room temperature). This means that no more than 6 mg/kg are injected in a standard 70 kg human, which is also well below the LD_{50} for ethanol administered i.v. in rats (1440 mg/kg[116]). So, even knowing that ethanol represents 5% of total [^{11}C]PiB final solution there is no risk in its administration to humans. In fact our 5% of ethanol

are below the 10% limit used in several radiopharmaceutical centres to enhance the solubility of highly lipophilic radiotracers or to decrease their adsorption to vials, membrane filters, and syringes[117]. As a precaution to the potential side effects of ethanol (pain and haemolysis) the solution should be injected slowly, which decreases the concentration at the site of injection by rapid mixing with large volumes of blood.

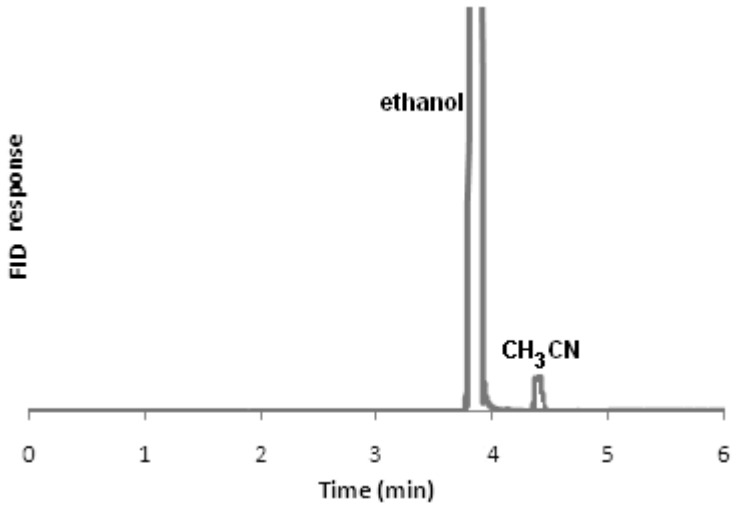

Figure 5.11. Gas chromatography of the final [^{11}C]PiB i.v. solution.

For quantifying chemical and radiochemical purity we used a HPLC with a UV and radiometric detector. Although retention time of each chemical species have been previously identified by injection of cold standards, it was also injected into the HPLC an unpurified reaction crude mixture to ensure that each one would be effectively distinguished in this analytical method (see Figure 5.12).

Radiochemical purity is defined as the percentage of the radionuclide present in the desired chemical form whereas chemical purity refers to the proportion of the solution that is in a specific chemical form, regardless of the presence of radioactivity[114]. Radiochemical species are chromatographly separated based on differences in chemical characteristics, then the radioactivity associated with each chemical species is assayed using a radiometric detector. Generally chemical impurities in radiotracer preparations only are problematic if they are toxic, can cause undesired interactions or modify the physiological process under study. That is why, although radiochemical

purity for i.v. doses typically must be higher than 95%, there are currently no chemical purity requirements for release of radiotracers for clinical use[102].

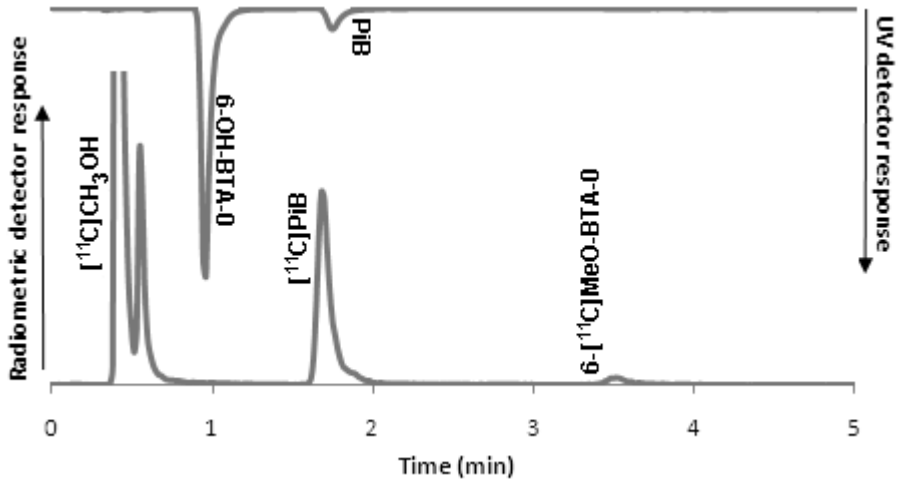

Figure 5.12. Analytical HPLC of [^{11}C]PiB solution before purification.

All [^{11}C]PiB final solutions controlled have revealed a level of radiochemical purity ≥98% and chemical purity >95% (see Table 5.5), as can be seen on Figure 5.13 by the presence of a single species in a typical chromatogram before i.v. administration. Radiochemical identity of [^{11}C]PiB can be confirmed by comparison of its r_t with the one obtained with the cold reference standard or by co-injection in the analytical HPLC.

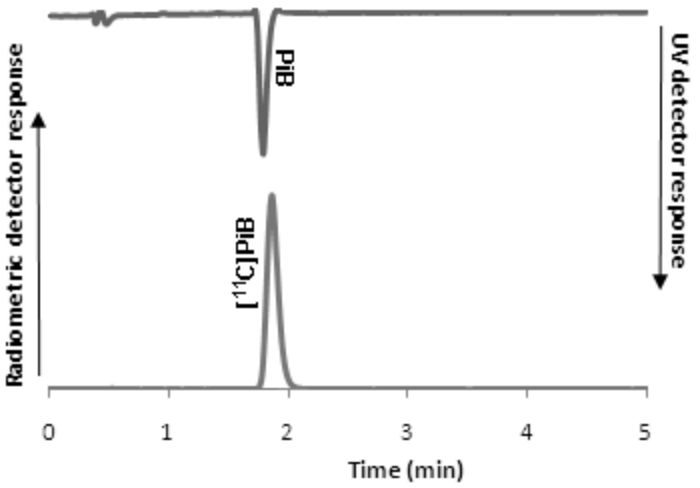

Figure 5.13. Analytical HPLC of the final [^{11}C]PiB i.v. solution.

It should be noted that radiochemical purity may not be constant since it has been recognized that aqueous solutions of radiolabelled compounds tend to decompose when exposed to high temperatures, when comes into contact with the final vial rubber stopper components or over time via radiolysis caused by the interaction of their own radiation with water[114, 118]. However, a sample of our product placed in contact with the butyl rubber stopper showed, after 3 hours, to continue with a radiochemical purity higher than 98%. The same happened when it was submitted to an autoclaving process that reaches a temperature between 131.5º-132.5º C during 2 minutes, which proved the great stability of this radiotracer. A study over time also demonstrated that the radiotracer is stable at least 4 hours after synthesis at room temperature, having a radiochemical purity above 97% (see Figure 5.14).

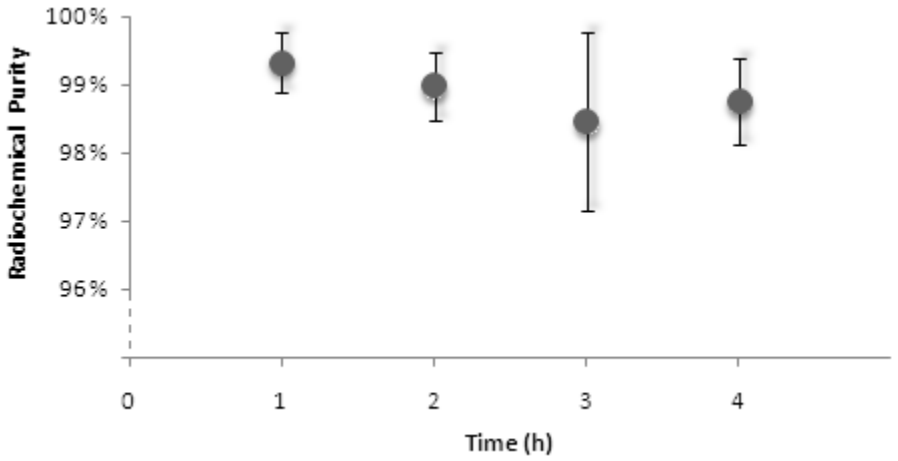

Figure 5.14. [^{11}C]PiB final solution stability over time.

The intensity of radiolysis is extremely dependent on the amount of final activity obtained and on the radiotracer SA[114, 118]. The value of this latter parameter is calculated using a reference curve (see Figure 5.3) and the known total activity and final volume of [^{11}C]PiB solution. The achieved SA (EOS) is in the range of 27.6±4.1 GBq/µmol which, as already discussed above, is suitable for human molecular imaging studies.

Through SA and total EOS activity is possible to estimate the number of moles and consequently the mass of PiB present in solution (MM = 256 g/mol). By this way we can arrive to an important parameter to be taken into account in injectable solutions,

the osmolarity, which measures the number of moles of a chemical compound per litre that contributes to osmotic pressure. This process is of vital importance once cell membranes are selective according to the solutes found in circulation. The osmolarity of the i.v. agents should also be appropriate for blood in order to not cause haemolysis and, for this reason, it should be taken into account the reference value of NaCl 0.9% osmolarity (approx. 308 mOsmol/liter).

A theoretical osmolarity concentration can be calculated for [^{11}C]PiB solution using the equation mOsmol/liter = [(mass (g)/volume (l)) / MM (g/mol)] x (nº of species x 1000). Considering the mean values of total activity EOS (3.2 GBq) and SA (27.6 GBq/µmol), knowing that our final volume is 10 ml (0.5 ml of ethanol and 9.5 ml of NaCl 0.9%) and since there is no dissociation of the compound it was reached a theoretical value of approximately 0.012 mOsmol/liter for [^{11}C]PiB solution. So, the contribution of this value would not significantly affect the isotonicity and osmolarity of the principal vehicle for injection (NaCl 0.9%) since ethanol is not taken into account as it freely diffuses through the cell membrane.

Sterile filter integrity test also gives some assurances about the quality of the solution injected and later tests for bacterial endotoxins (LAL test) always demonstrated that it had less than 17.5 EU/ml, as specified in Ph. Eur. However, because short lived radiotracers cannot be tested for all pharmaceutical parameters prior to administration, the entire process must be monitored and documented.

In conclusion, the whole procedure from the release of [^{11}C]CO_2 by cyclotron to final i.v. administration of the radiotracer, including quality control, is performed in about 45 minutes. This time is clearly compatible with radioisotope $t_{1/2}$ avoiding excessive losses in its radioactivity.

6. Final considerations

Due to the socio-economic impact and the alarming increase in its incidence in modern societies, largely because the demographic transition that has been observed in recent decades with repercussions in population aging, AD has been the target of a huge scientific investment for its understanding. Constantly new findings are being revealed that lead to a better understanding of this dementia, such as a recent study that provided evidences that Aβ protein aggregates can behave as prions (infectious agent composed by abnormal proteins) that cause AD[119] or another one that showed that a mutation in the APP A673T gene confers a protective effect against it[120].

In the absence of a curative or preventive treatment for AD, an early diagnosis allows a non-pharmacological and pharmacological intervention focusing in relieving symptoms and preserving physical skills, with real gains in quality of life. So, highly specific and sensitive biomarkers are of great value to assess an early diagnosis that could result in therapeutic efficacy. However, initial identification of typical AD molecular changes generally involves techniques that are not widely disseminated and that, in some cases, are also complex and invasive.

In an attempt to counter these assumptions efforts were made in the area of Molecular Imaging that led to the development of [^{11}C]PiB, a promising PET agent that has been widely used since the beginning of the XXI century. Its efficiency for the early detection of Aβ, characteristic of AD, and differentiation from other dementias continues to be reiterated by recent studies that support the idea that this radiotracer is particularly useful as a diagnostic tool for distinguish AD from prodromal or MCI stages and also could be useful for the discovery of novel disease-related properties of amyloid[121]. The interest in the use of [^{11}C]PiB has been such that the limits on its use exceeded the boundaries of AD since, for example, there are recent data that suggest its potential in the quantification of demyelination in multiple sclerosis patients[122].

Despite the affinity, specificity and sensitivity demonstrated for earlier detection of Aβ plaques, due to the limited half-life, [^{11}C]PiB can only be used at sites that have the unavoidable conditions for its production, including a radiochemistry laboratory with cyclotron, and detection by PET, which has hindered the access of the general population for this diagnostic exam. By having all these conditions, ICNAS made a strong commitment to establish an automated and reproducible process for radiolabelling, purification and reformulation of [^{11}C]PiB using a system composed by

commercial synthesis modules (Bioscan Inc.) in order to obtain a sterile and pyrogen-free injectable solution to be used in humans. The advantages of using automated synthesis modules over more traditional approaches are related to a more reliable reproducibility of the process, to a safer and facilitated handling of high radioactivity doses by eliminating manual operations and with the regulatory compliance with pharmaceutical manufacturing practices.

The used captive solvent [^{11}C]methylation method have proved to be extremely effective for [^{11}C]PiB radiosynthesis presenting, after optimization, an absolute reaction yield of 23.5±6.8%, a SA of 27.6±4.1 GBq/µmol, and a radiochemical purity of at least 98%. These aspects were confirmed *in vivo* by human clinical assays where, confronting healthy persons with patients whose history refers to a suspected AD, it was observed a hiperfixation in the characteristic regions of this dementia (frontoparietal lobes) and very low uptake in control cases (see Figure 6.1).

Despite its effectiveness, one of the major drawbacks of the method used is that radiotracers coexist with a reasonable high quantity of the non-radioactive species, leading to limited specific activities. In this work we tried to reduce to the maximum possible the formation of non-radioactive species due to the presence and incorporation of atmospheric [^{12}C]CO_2 before treatment with HI. However, other factors as increasing cyclotron target gas purity (e.g., through filtration), the use of a more concentrated $LiAlH_4$/THF solution (1 M) or, although more difficult because it requires quite different equipment, a [^{11}C]CH_3I production by the “gas phase” method, may be procedures that could be tested in future to increase SA.

The performed optimization in [^{11}C]PiB radiosynthesis also served to prepare all the system and refine techniques that could lead to the availability of other carbon-11 radiotracers for clinical assays in ICNAS (e.g., [^{11}C]PK11195, [^{11}C]raclopride or [^{11}C]flumazenil) or for the development of new radiolabelled molecules.

Regardless of compelling results with [^{11}C]PIB the short half-life limits the use of [^{11}C]molecules. This emphasizes the need for [^{18}F]molecules, with longer half-life, to implement a broader Aβ PET imaging. The radiotracers for AD that have been developed to date have focused primarily on the affinity for the Aβ deposits. However it is known that there are several subspecies of Aβ whose importance is still not fully known since there are cases of dementia symptoms without the associated plaques and there are also cases in which the presence of these are not manifested symptomatically.

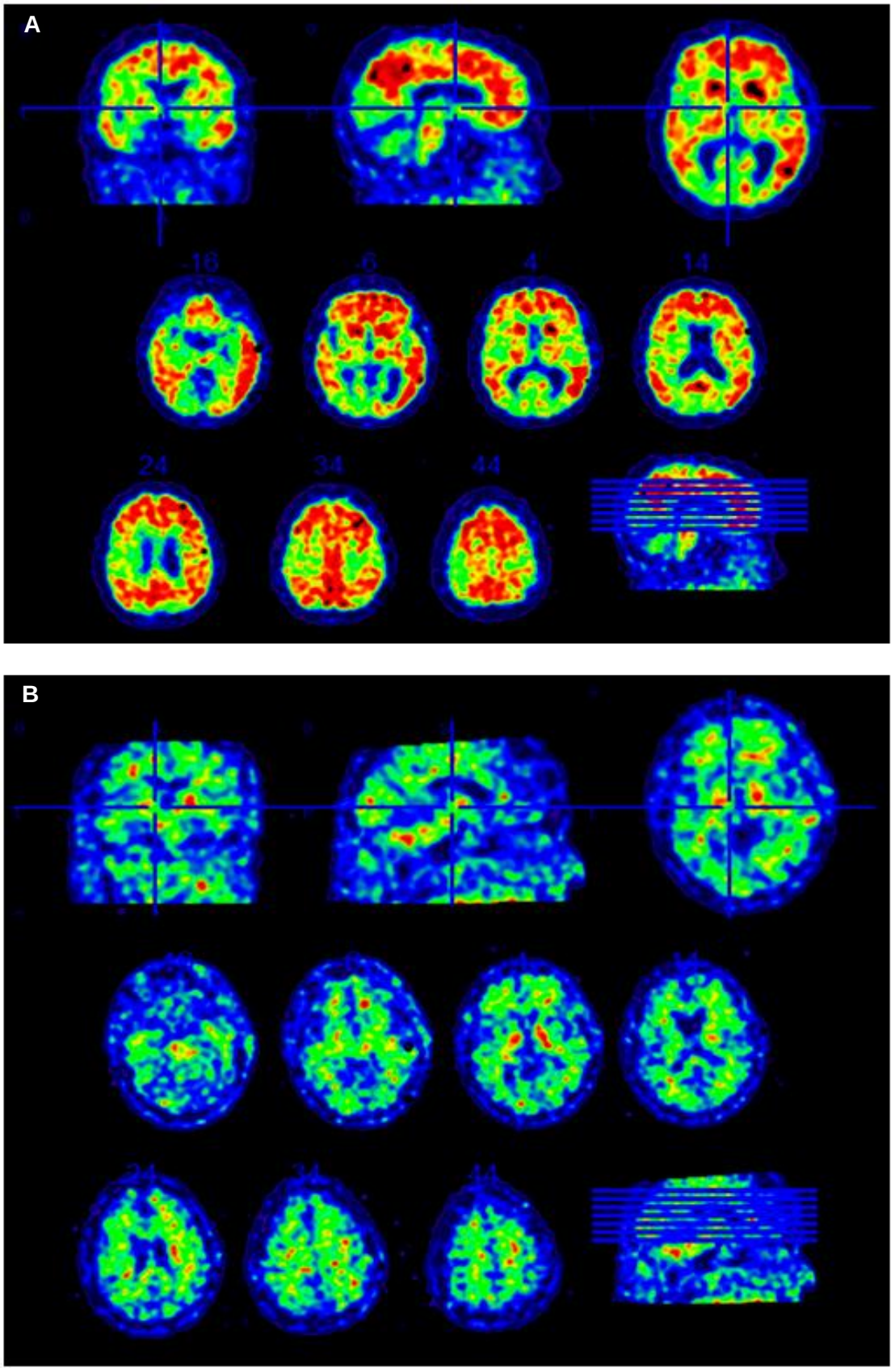

Figure 6.1. [^{11}C]PiB amyloid binding to the brain of an AD (A) and healthy (B) cases. Red indicates high, green medium and blue low [^{11}C]PiB retention. (Images courtesy of ICNAS)

A challenge that has been stimulating the radiochemical community, involves the synthesis of radiotracers that allow visualizing *in vivo* the different Aβ subspecies and its expression in the brain with and without pathology. Thus, amyloid imaging may become more and more a sensitive tool for the early detection of AD. This could assist in the selection of patients for anti-amyloid therapies and help to better understand the underlying pathological mechanisms and progression of this dementia.

Beyond the development of new specific radiotracers it is also important to recognize the utility of the new hybrid systems, in particular PET/MRI, since these add a tremendous spatial resolution to molecular imaging allowing the revelation of critical information regarding to early changes in the anatomy and physiology of dementia.

Together, the development of even more specific radiotracers and the tuning of the detection technology, may lead to a change in the paradigm of the early diagnosis and potential treatment of Alzheimer's disease. The truth is that, more than ever, this pathology is on the scientific worldwide agenda and we are heading for a broader comprehension of its very primordial molecular mechanisms.

7.References

1. Hayashi C, Olkkonen H, Sikken B, Yermo J. Transforming Pensions and Healthcare in a Rapidly Ageing World: Opportunities and Collaborative Strategies. World Scenario Series. 2009.
2. Prince M, Bryce R, Ferri C. World Alzheimer Report 2011: The benefits of early diagnosis and intervention. 2011.
3. Brookmeyer R, Johnson E, Ziegler-Graham K, Arrighi HM. Forecasting the global burden of Alzheimer's disease. Alzheimers Dement. 2007;3(3):186-91.
4. Chiara F, Daniela G, Elio S. Genetics and Molecular Biology of Alzheimer's Disease and Frontotemporal Lobar Degeneration. Eur Neur Rev. 2010;5(1):12-6.
5. Kilbourn MR, Snyder SE, Sherman PS, Kuhl DE. In vivo studies of acetylcholinesterase activity using a labeled substrate, N-[11C]methylpiperdin-4-yl propionate ([11C]PMP). Synapse. 1996;22(2):123-31.
6. Herholz K, Carter SF, Jones M. Positron emission tomography imaging in dementia. Br J Radiol. 2007;80(Spec No 2):S160-7.
7. Streit WJ. Microglia and Alzheimer's disease pathogenesis. J Neurosci Res. 2004;77(1):1-8.
8. Mattson MP. Pathways towards and away from Alzheimer's disease. Nature. 2004;430(7000):631-9.
9. Alzheimer A. Über eine eigenartige Erkrankung der Hirnrinde (1907). About a peculiar disease of the cerebral cortex (Translated by L. Jarvik and H. Greenson). Alzheimer Dis Assoc Disord. 1987;1(1):3-8.
10. Ballard C, Gauthier S, Corbett A, Brayne C, Aarsland D, Jones E. Alzheimer's disease. Lancet. 2011;377(9770):1019-31. Epub 2011 Mar 1.
11. Yankner BA, Duffy LK, Kirschner DA. Neurotrophic and neurotoxic effects of amyloid beta protein: reversal by tachykinin neuropeptides. Science. 1990;250(4978):279-82.
12. Lambert MP, Barlow AK, Chromy BA, Edwards C, Freed R, Liosatos M, et al. Diffusible, nonfibrillar ligands derived from Abeta1-42 are potent central nervous system neurotoxins. Proc Natl Acad Sci U S A. 1998;95(11):6448-53.
13. Kayed R, Head E, Thompson JL, McIntire TM, Milton SC, Cotman CW, et al. Common structure of soluble amyloid oligomers implies common mechanism of pathogenesis. Science. 2003;300(5618):486-9.
14. Hardy J. Has the amyloid cascade hypothesis for Alzheimer's disease been proved? Curr Alzheimer Res. 2006;3(1):71-3.
15. Small SA, Gandy S. Sorting through the cell biology of Alzheimer's disease: intracellular pathways to pathogenesis. Neuron. 2006;52(1):15-31.
16. Small SA, Duff K. Linking Abeta and tau in late-onset Alzheimer's disease: a dual pathway hypothesis. Neuron. 2008;60(4):534-42.
17. Meraz-Rios MA, Lira-De Leon KI, Campos-Pena V, De Anda-Hernandez MA, Mena-Lopez R. Tau oligomers and aggregation in Alzheimer's disease. J Neurochem. 2010;112(6):1353-67. Epub 2009 Nov 27.
18. Holes C, Wilkinson D. Molecular biology of Alzheimer's disease. Adv Psy Treat. 2000;6:193-200.
19. Lovestone S, Anderton B. Cytoskeletal abnormalities in Alzheimer's disease. Curr Opin Neurol Neurosurg. 1992;5(6):883-8.
20. Ertekin-Taner N. Genetics of Alzheimer disease in the pre- and post-GWAS era. Alzheimers Res Ther. 2010;2(1):3.
21. Bertram L, McQueen MB, Mullin K, Blacker D, Tanzi RE. Systematic meta-analyses of Alzheimer disease genetic association studies: the AlzGene database. Nat Genet. 2007;39(1):17-23.
22. Morris HR, Lees AJ, Wood NW. Neurofibrillary tangle parkinsonian disorders--tau pathology and tau genetics. Mov Disord. 1999;14(5):731-6.

23. Raghavan R, Khin-Nu C, Brown AG, Day KA, Tyrer SP, Ince PG, et al. Gender differences in the phenotypic expression of Alzheimer's disease in Down's syndrome (trisomy 21). Neuroreport. 1994;5(11):1393-6.

24. Dubois B, Feldman H, Jacova C, Dekosky S, Barberger-Gateau P, Cummings J, et al. Research criteria for the diagnosis of Alzheimer's disease: revising the NINCDS-ADRDA criteria. Lancet Neurol. 2007;6(8):734-46.

25. Waldemar G, Dubois B, Emre M, Georges J, McKeith IG, Rossor M, et al. Recommendations for the diagnosis and management of Alzheimer's disease and other disorders associated with dementia: EFNS guideline. Eur J Neurol. 2007;14(1):e1-26.

26. Hejl A, Hogh P, Waldemar G. Potentially reversible conditions in 1000 consecutive memory clinic patients. J Neurol Neurosurg Psychiatry. 2002;73(4):390-4.

27. Clarfield AM. The decreasing prevalence of reversible dementias: an updated meta-analysis. Arch Intern Med. 2003;163(18):2219-29.

28. Kloppel S, Stonnington CM, Chu C, Draganski B, Scahill RI, Rohrer JD, et al. Automatic classification of MR scans in Alzheimer's disease. Brain. 2008;131(Pt 3):681-9. Epub 2008 Jan 17.

29. Costa D, Oliveira J, Bressanc R. PET e SPECT em neurologia e psiquiatria: do básico às aplicações clínicas. Rev Bras Psiquiatr. 2001;23(Supl I):4-5.

30. Kadir A, Nordberg A. Target-specific PET probes for neurodegenerative disorders related to dementia. J Nucl Med. 2010;51(9):1418-30.

31. Patwardhan MB, McCrory DC, Matchar DB, Samsa GP, Rutschmann OT. Alzheimer disease: operating characteristics of PET--a meta-analysis. Radiology. 2004;231(1):73-80. Epub 2004 Feb 27.

32. Wagner H, Buchanan J, Szabo Z. Principles of Nuclear Medicine 2nd ed. WB Saunders, Philadelphia: Elsevier Health Sciences; 1995.

33. Vallabhajosula S. Molecular Imaging: Radiopharmaceuticals for PET and SPECT. 1st ed. Berlin, Germany: Springer-Verlag; 2009.

34. Kung HF, Ohmomo Y, Kung MP. Current and future radiopharmaceuticals for brain imaging with single photon emission computed tomography. Semin Nucl Med. 1990;20(4):290-302.

35. Saha GB, MacIntyre WJ, Go RT. Radiopharmaceuticals for brain imaging. Semin Nucl Med. 1994;24(4):324-49.

36. Lee Y. Radiopharmaceuticals for Molecular Imaging. Open Nucl Med J. 2010;2:178-85.

37. Clemente G. Estudo Comparativo de Procedimentos Experimentais e Computacionais para Cálculo da Lipofilia Molecular. Saúde & Tecnologia. 2011;5:29-34.

38. Nagren K, Halldin C, Rinne JO. Radiopharmaceuticals for positron emission tomography investigations of Alzheimer's disease. Eur J Nucl Med Mol Imaging. 2010;37(8):1575-93. Epub 2009 Dec 22.

39. Nobili F, Koulibaly PM, Rodriguez G, Benoit M, Girtler N, Robert PH, et al. 99mTc-HMPAO and 99mTc-ECD brain uptake correlates of verbal memory in Alzheimer's disease. Q J Nucl Med Mol Imaging. 2007;51(4):357-63.

40. Cohen MB, Graham LS, Lake R, Metter EJ, Fitten J, Kulkarni MK, et al. Diagnosis of Alzheimer's disease and multiple infarct dementia by tomographic imaging of iodine-123 IMP. J Nucl Med. 1986;27(6):769-74.

41. Zipser BD, Johanson CE, Gonzalez L, Berzin TM, Tavares R, Hulette CM, et al. Microvascular injury and blood-brain barrier leakage in Alzheimer's disease. Neurobiol Aging. 2007;28(7):977-86. Epub 2006 Jun 16.

42. Raichle ME, Martin WR, Herscovitch P, Mintun MA, Markham J. Brain blood flow measured with intravenous H2(15)O. II. Implementation and validation. J Nucl Med. 1983;24(9):790-8.

43. Clerici F, Del Sole A, Chiti A, Maggiore L, Lecchi M, Pomati S, et al. Differences in hippocampal metabolism between amnestic and non-amnestic MCI subjects: automated FDG-PET image analysis. Q J Nucl Med Mol Imaging. 2009;53(6):646-57. Epub 2009 Oct 7.

44. Morbelli S, Piccardo A, Villavecchia G, Dessi B, Brugnolo A, Piccini A, et al. Mapping brain morphological and functional conversion patterns in amnestic MCI: a voxel-based MRI and FDG-PET study. Eur J Nucl Med Mol Imaging. 2010;37(1):36-45. Epub .

45. Jacobs AH, Winkler A, Castro MG, Lowenstein P. Human gene therapy and imaging in neurological diseases. Eur J Nucl Med Mol Imaging. 2005;32(Suppl 2):S358-83.

46. Saha G. Fundamentals of Nuclear Pharmacy. 6th ed. New York, EUA: Springer-Verla; 2010.

47. Ryan D. Misdiagnosis in dementia: comparisons of diagnostic error rate and range of hospital investigation according to medical specialty. Int J Geriatr Psychiatry. 1994;9:141-47.

48. Nordberg A, Lundqvist H, Hartvig P, Lilja A, Langstrom B. Kinetic analysis of regional (S)(-)11C-nicotine binding in normal and Alzheimer brains--in vivo assessment using positron emission tomography. Alzheimer Dis Assoc Disord. 1995;9(1):21-7.

49. Sabri O, Kendziorra K, Wolf H, Gertz HJ, Brust P. Acetylcholine receptors in dementia and mild cognitive impairment. Eur J Nucl Med Mol Imaging. 2008;35(Suppl 1):S30-45.

50. Namba H, Irie T, Fukushi K, Iyo M. In vivo measurement of acetylcholinesterase activity in the brain with a radioactive acetylcholine analog. Brain Res. 1994;667(2):278-82.

51. Silverman DHS. PET in the Evaluation of Alzheimer's Disease and Related Disorders. 1st ed. New York, USA: Springer; 2009.

52. Small GW, Kepe V, Ercoli LM, Siddarth P, Bookheimer SY, Miller KJ, et al. PET of brain amyloid and tau in mild cognitive impairment. N Engl J Med. 2006;355(25):2652-63.

53. Rowe CC, Ackerman U, Browne W, Mulligan R, Pike KL, O'Keefe G, et al. Imaging of amyloid beta in Alzheimer's disease with 18F-BAY94-9172, a novel PET tracer: proof of mechanism. Lancet Neurol. 2008;7(2):129-35. Epub 2008 Jan 10.

54. Ikonomovic MD, Klunk WE, Abrahamson EE, Mathis CA, Price JC, Tsopelas ND, et al. Post-mortem correlates of in vivo PiB-PET amyloid imaging in a typical case of Alzheimer's disease. Brain. 2008;131(Pt 6):1630-45. Epub 2008 Mar 12.

55. Lopresti BJ, Klunk WE, Mathis CA, Hoge JA, Ziolko SK, Lu X, et al. Simplified quantification of Pittsburgh Compound B amyloid imaging PET studies: a comparative analysis. J Nucl Med. 2005;46(12):1959-72.

56. Klunk WE, Engler H, Nordberg A, Wang Y, Blomqvist G, Holt DP, et al. Imaging brain amyloid in Alzheimer's disease with Pittsburgh Compound-B. Ann Neurol. 2004;55(3):306-19.

57. Klunk WE, Wang Y, Huang GF, Debnath ML, Holt DP, Shao L, et al. The binding of 2-(4'-methylaminophenyl)benzothiazole to postmortem brain homogenates is dominated by the amyloid component. J Neurosci. 2003;23(6):2086-92.

58. Okamura N, Yanai K. Florbetapir (18F), a PET imaging agent that binds to amyloid plaques for the potential detection of Alzheimer's disease. IDrugs. 2010;13(12):890-9.

59. Thompson PW, Ye L, Morgenstern JL, Sue L, Beach TG, Judd DJ, et al. Interaction of the amyloid imaging tracer FDDNP with hallmark Alzheimer's disease pathologies. J Neurochem. 2009;109(2):623-30. Epub 2009 Feb 13.

60. Lowe VJ, Kemp BJ, Jack CR, Jr., Senjem M, Weigand S, Shiung M, et al. Comparison of 18F-FDG and PiB PET in cognitive impairment. J Nucl Med. 2009;50(6):878-86. Epub 2009 May 14.

61. Rabinovici GD, Rosen HJ, Alkalay A, Kornak J, Furst AJ, Agarwal N, et al. Amyloid vs FDG-PET in the differential diagnosis of AD and FTLD. Neurology. 2011;77(23):2034-42. Epub 11 Nov 30.

62. Lockhart A, Lamb JR, Osredkar T, Sue LI, Joyce JN, Ye L, et al. PIB is a non-specific imaging marker of amyloid-beta (Abeta) peptide-related cerebral amyloidosis. Brain. 2007;130(Pt 10):2607-15. Epub 007 Aug 13.

63. Noda A, Murakami Y, Nishiyama S, Fukumoto D, Miyoshi S, Tsukada H, et al. Amyloid imaging in aged and young macaques with [11C]PIB and [18F]FDDNP. Synapse. 2008;62(6):472-5.

64. Quigley H, Colloby SJ, O'Brien JT. PET imaging of brain amyloid in dementia: a review. Int J Geriatr Psychiatry. 2010;26:991-99.

65. Wong DF, Rosenberg PB, Zhou Y, Kumar A, Raymont V, Ravert HT, et al. In vivo imaging of amyloid deposition in Alzheimer disease using the radioligand 18F-AV-45 (florbetapir [corrected] F 18). J Nucl Med. 2010;51(6):913-20.

66. Raji CA, Becker JT, Tsopelas ND, Price JC, Mathis CA, Saxton JA, et al. Characterizing regional correlation, laterality and symmetry of amyloid deposition in mild cognitive impairment and Alzheimer's disease with Pittsburgh Compound B. J Neurosci Methods. 2008;172(2):277-82. Epub 2008 May 16.

67. Boellaard R, O'Doherty MJ, Weber WA, Mottaghy FM, Lonsdale MN, Stroobants SG, et al. FDG PET and PET/CT: EANM procedure guidelines for tumour PET imaging: version 1.0. Eur J Nucl Med Mol Imaging. 2010;37(1):181-200.

68. Alzheimer's Disease Neuroimaging Initiative. PET Technical Procedures Manual: Supplemental Imaging Protocol Using Pittsburgh Compound B (PiB) v1.2. 2007.

69. Fodero-Tavoletti MT, Rowe CC, McLean CA, Leone L, Li QX, Masters CL, et al. Characterization of PiB binding to white matter in Alzheimer disease and other dementias. J Nucl Med. 2009;50(2):198-204. Epub 2009 Jan 21.

70. Rostomian AH, Madison C, Rabinovici GD, Jagust WJ. Early 11C-PIB frames and 18F-FDG PET measures are comparable: a study validated in a cohort of AD and FTLD patients. J Nucl Med. 2011;52(2):173-9. Epub 2011 Jan 13.

71. Yousefi BH, Manook A, Drzezga A, von Reutern B, Schwaiger M, Wester HJ, et al. Synthesis and evaluation of 11C-labeled imidazo[2,1-b]benzothiazoles (IBTs) as PET tracers for imaging beta-amyloid plaques in Alzheimer's disease. J Med Chem. 2011;54(4):949-56. Epub 2011 Jan 28.

72. Nordberg A, Rinne JO, Kadir A, Langstrom B. The use of PET in Alzheimer disease. Nat Rev Neurol. 2010;6(2):78-87.

73. Nordberg A. PET imaging of amyloid in Alzheimer's disease. Lancet Neurol. 2004;3(9):519-27.

74. Scheinin NM, Aalto S, Koikkalainen J, Lotjonen J, Karrasch M, Kemppainen N, et al. Follow-up of [11C]PIB uptake and brain volume in patients with Alzheimer disease and controls. Neurology. 2009;73(15):1186-92. Epub 2009 Sep 2.

75. Langstrom B, Andren PE, Lindhe O, Svedberg M, Hall H. In vitro imaging techniques in neurodegenerative diseases. Mol Imaging Biol. 2007;9(4):161-75.

76. Petersen R, Morris J. Mild Cognitive Impairment: Aging to Alzheimer’s disease. 1st ed. New York: Oxford University Press, Inc.; 2003.

77. Ng S, Villemagne VL, Berlangieri S, Lee ST, Cherk M, Gong SJ, et al. Visual assessment versus quantitative assessment of 11C-PIB PET and 18F-FDG PET for detection of Alzheimer's disease. J Nucl Med. 2007;48(4):547-52.

78. Miller PW, Long NJ, Vilar R, Gee AD. Synthesis of 11C, 18F, 15O, and 13N radiolabels for positron emission tomography. Angew Chem Int Ed Engl. 2008;47(47):8998-9033.

79. Schlyer DJ. PET tracers and radiochemistry. Ann Acad Med Singapore. 2004;33(2):146-54.

80. Li Z, Conti PS. Radiopharmaceutical chemistry for positron emission tomography. Adv Drug Deliv Rev. 2010;62(11):1031-51. Epub 2010 Sep 18.

81. Schubiger P, Lehmann L, Friebe M. PET Chemistry The drive force in molecular imaging. 1st ed. Berlin, Germany: Springer-Verlag; 2007.

82. Allard M, Fouquet E, James D, Szlosek-Pinaud M. State of art in 11C labelled radiotracers synthesis. Curr Med Chem. 2008;15(3):235-77.

83. Kniess T, Rode K, Wuest F. Practical experiences with the synthesis of [11C]CH3I through gas phase iodination reaction using a TRACERlabFXC synthesis module. Appl Radiat Isot. 2008;66(4):482-8. Epub 2007 Jun 27.

84. Scott PJ. Methods for the incorporation of carbon-11 to generate radiopharmaceuticals for PET imaging. Angew Chem Int Ed Engl. 2009;48(33):6001-4.

85. Nagren K, Halldin C, Muller L, Swahn CG, Lehikoinen P. Comparison of [11C]methyl triflate and [11C]methyl iodide in the synthesis of PET radioligands such as [11C]beta-CIT and [11C]beta-CFT. Nucl Med Biol. 1995;22(8):965-79.

86. Nagren K, Muller L, Halldin C, Swahn CG, Lehikoinen P. Improved synthesis of some commonly used PET radioligands by the use of [11C]methyl triflate. Nucl Med Biol. 1995;22(2):235-9.

87. Jewett DM. A simple synthesis of [11C]methyl triflate. Int J Rad Appl Instrum A. 1992;43(11):1383-5.

88. Wilson AA, Garcia A, Houle S, Vasdev N. Utility of commercial radiosynthetic modules in captive solvent [11C]-methylation reactions. 2009.

89. Wilson AA, Garcia A, Jin L, Houle S. Radiotracer synthesis from [(11)C]-iodomethane: a remarkably simple captive solvent method. Nucl Med Biol. 2000;27(6):529-32.

90. Jacobson O, Mishani E. [11C]-dimethylamine as a labeling agent for PET biomarkers. Appl Radiat Isot. 2008;66(2):188-93. Epub 2007 Aug 30.

91. Hamill TG, Krause S, Ryan C, Bonnefous C, Govek S, Seiders TJ, et al. Synthesis, characterization, and first successful monkey imaging studies of metabotropic glutamate receptor subtype 5 (mGluR5) PET radiotracers. Synapse. 2005;56(4):205-16.

92. LeVine H, 3rd. Quantification of beta-sheet amyloid fibril structures with thioflavin T. Methods Enzymol. 1999;309:274-84.

93. Klunk WE, Wang Y, Huang GF, Debnath ML, Holt DP, Mathis CA. Uncharged thioflavin-T derivatives bind to amyloid-beta protein with high affinity and readily enter the brain. Life Sci. 2001;69(13):1471-84.

94. Mathis CA, Bacskai BJ, Kajdasz ST, McLellan ME, Frosch MP, Hyman BT, et al. A lipophilic thioflavin-T derivative for positron emission tomography (PET) imaging of amyloid in brain. Bioorg Med Chem Lett. 2002;12(3):295-8.

95. Klunk WE, Mathis CA. Whatever happened to Pittsburgh Compound-A? Alzheimer Dis Assoc Disord. 2008;22(3):198-203.

96. Mathis CA, Wang Y, Holt DP, Huang GF, Debnath ML, Klunk WE. Synthesis and evaluation of 11C-labeled 6-substituted 2-arylbenzothiazoles as amyloid imaging agents. J Med Chem. 2003;46(13):2740-54.

97. Wilson AA, Garcia A, Chestakova A, Kung H, Houle S. A rapid one-step radiosynthesis of the β-amyloid imaging radiotracer N-methyl-[11C]2-(4′-methylaminophenyl)-6-hydroxybenzothiazole ([11C]-6-OH-BTA-1). J Label Compd Radiopharm. 2004;47:679-82.

98. Mikhno A, Devanand D, Pelton G, Cuasay K, Gunn R, Upton N, et al. Voxel-based analysis of 11C-PIB scans for diagnosing Alzheimer's disease. J Nucl Med. 2008;49(8):1262-9. Epub 2008 Jul 16.

99. Cheung MK, Ho CL. A simple, versatile, low-cost and remotely operated apparatus for [11C]acetate, [11C]choline, [11C]methionine and [11C]PIB synthesis. Appl Radiat Isot. 2009;67(4):581-9. Epub 2008 Dec 24.

100. Philippe C, Haeusler D, Mitterhauser M, Ungersboeck J, Viernstein H, Dudczak R, et al. Optimization of the radiosynthesis of the Alzheimer tracer 2-(4-N-[11C]methylaminophenyl)-6-hydroxybenzothiazole ([11C]PIB). Appl Radiat Isot. 2011;69(9):1212-7. Epub 2011 Apr 29.

101. Gomez-Vallejo V, Llop J. Fully automated and reproducible radiosynthesis of high specific activity [^{11}C]raclopride and [^{11}C]Pittsburgh Compound-B using the combination of two commercial synthesizers. Nucl Med Commun. 2011;32(11):1011-7.

102. Shao X, Hoareau R, Runkle AC, Tluczek LJM, Hockley BG, Henderson BD, et al. Highlighting the versatility of the Tracerlab synthesis modules. Part 2: fully automated production of [11C]-labeled radiopharmaceuticals using a Tracerlab FXC-Pro. 2011.

103. Solbach C, Uebele M, Reischl G, Machulla HJ. Efficient radiosynthesis of carbon-11 labelled uncharged Thioflavin T derivatives using [11C]methyl triflate for beta-amyloid imaging in Alzheimer's Disease with PET. Appl Radiat Isot. 2005;62(4):591-5.

104. Verdurand M, Bort G, Tadino V, Bonnefoi F, Le Bars D, Zimmer L. Automated radiosynthesis of the Pittsburg compound-B using a commercial synthesizer. Nucl Med Commun. 2008;29(10):920-6.

105. Gomez-Vallejo V, Llop J. Specific activity of [11C]CH3I synthesized by the "wet" method: main sources of non-radioactive carbon. Appl Radiat Isot. 2009;67(1):111-4. Epub 2008 Oct 5.

106. Crouzel C, Långström B, Pike VW, Coenen HH. Recommendations for a practical production of [11C]methyl iodide. International Journal of Radiation Applications and Instrumentation Part A Applied Radiation and Isotopes. 1987;38(8):601-3.

107. Langstrom B, Lundqvist H. The preparation of 11C-methyl iodide and its use in the synthesis of 11C-methyl-L-methionine. Int J Appl Radiat Isot. 1976;27(7):357-63.

108. Iwata R, Ido T, Ujiie A, Takahashi T, Ishiwata K, Hatano K, et al. Comparative study of specific activity of [11C]methyl iodide: A search for the source of carrier carbon. International Journal of Radiation Applications and Instrumentation Part A Applied Radiation and Isotopes. 1988;39(1):1-7.

109. Matarrese M, Soloviev D, Todde S, Neutro F, Petta P, Carpinelli A, et al. Preparation of [11C] radioligands with high specific radioactivity on a commercial PET tracer synthesizer. Nucl Med Biol. 2003;30(1):79-83.

110. Klein AT, Holschbach M. Labelling of the solvent DMSO as side reaction of methylations with n.c.a. [11C]CH3I. Appl Radiat Isot. 2001;55(3):309-13.

111. Iwata R, Pascali C, Bogni A, Miyake Y, Yanai K, Ido T. A simple loop method for the automated preparation of (11C)raclopride from (11C)methyl triflate. Appl Radiat Isot. 2001;55(1):17-22.

112. Serdons K, Verduyckt T, Vanderghinste D, Borghgraef P, Cleynhens J, Van Leuven F, et al. 11C-labelled PIB analogues as potential tracer agents for in vivo imaging of amyloid beta in Alzheimer's disease. Eur J Med Chem. 2009;44(4):1415-26. Epub 2008 Oct 7.

113. Manook A, Yousefi BH, Willuweit A, Platzer S, Reder S, Voss A, et al. Small-animal PET imaging of amyloid-beta plaques with [11C]PiB and its multi-modal validation in an APP/PS1 mouse model of Alzheimer's disease. PLoS One. 2012;7(3):e31310. Epub 2012 Mar 9.

114. IAEA. Quality Assurance for Radioactivity Measurment in Nuclear Medicine. Technical Reports Series nº454. Vienna: International Atomic Energy Agency; 2006.

115. Hung JC. Comparison of various requirements of the quality assurance procedures for (18)F-FDG injection. J Nucl Med. 2002;43(11):1495-506.

116. Lewis RJ. Sax's Dangerous Properties of Industrial Materials. 9th ed. ed. New York: NY: Van Nostrand Reinhold; 1996.

117. Serdons K, Verbruggen A, Bormans G. The presence of ethanol in radiopharmaceutical injections. J Nucl Med. 2008;49(12):2071. Epub 08 Nov 7.

118. Fukumura T, Nakao R, Yamaguchi M, Suzuki K. Stability of 11C-labeled PET radiopharmaceuticals. Appl Radiat Isot. 2004;61(6):1279-87.

119. Stohr J, Watts JC, Mensinger ZL, Oehler A, Grillo SK, Dearmond SJ, et al. Purified and synthetic Alzheimer's amyloid beta (Abeta) prions. Proc Natl Acad Sci U S A. 2012;109(27):11025-30. Epub 2012 Jun 18.

120. Jonsson T, Atwal JK, Steinberg S, Snaedal J, Jonsson PV, Bjornsson S, et al. A mutation in APP protects against Alzheimer's disease and age-related cognitive decline. Nature. 2012;11(10).

121. Beckett TL, Webb RL, Niedowicz DM, Holler CJ, Matveev S, Baig I, et al. Postmortem Pittsburgh Compound B (PiB) Binding Increases with Alzheimer's Disease Progression. J Alzheimers Dis. 2012;5:5.

122. Jones N. Multiple sclerosis: Can Pittsburgh Compound B PET imaging quantify demyelination in MS? Nat Rev Neurol. 2011;7(1):2.